5-2021

Agreement Level of Running Temporal Measurements, Kinetics, and Force-Time Curves Calculated from Inertial Measurement Units

Austin Smith
East Tennessee State University

Agreement Level of Running Temporal Measurements, Kinetics, and Force-Time Curves Calculated from Inertial Measurement Units

---

A dissertation

presented to

the faculty of the Department of Sport, Exercise, Recreation and Kinesiology

East Tennessee State University

In partial fulfillment

of the requirements for the degree

Doctor of Philosophy in Sport Physiology and Performance

---

by

Austin Patrick Smith

May 2021

Dr. Brad DeWeese, Chair

Dr. Satoshi Mizuguchi

Dr. Matt Sams

Dr. Michael Stone

Keywords: two-mass model, inertial measurement units, force-time curves, gait events, impulses

ABSTRACT

Agreement Level of Running Temporal Measurements, Kinetics, and Force-Time Curves Calculated from Inertial Measurement Units

by

Austin Patrick Smith

Inertial measurement units (IMUs) and wearable sensors have enabled athlete monitoring and research to become more ecologically valid due to their small size and low cost. Under Specific conditions, IMUs and accelerometers have demonstrated high validity when measuring temporal gait event moments during upright running. While the use of IMUs has increased in the sport performance and athlete monitoring realm, the potential of the technology's ability to estimate running force-time curves utilizing the two-mass model (TMM) remains unexplored. The purpose of this study was to assess the agreement level of estimating temporal gait events and force-time curves from shank-mounted IMUs. Using the raw data from the IMUs, GCT, FT, total step time (ST), PF, and two-mass model-based force-time (F-t) curves were generated for 25 steps at 8 different speeds. Paired sample T-tests were performed on the gait events and peak force between the IMU and treadmill with both individual step comparison and averages per each speed. 95% confidence intervals were calculated for each timepoint of the force time curves. No statistically significant differences ($p > 0.05$) and nearly perfect relationships were observed for the step averages for each speed with FT, ST, and PF. Confidence intervals of the corrected mean difference suggest that F-t curves calculated from the TMM may not be valid when assessing the running population as a whole. In skilled runners, the 95% CI for the mean difference contained zero within the first 60% of the GCT duration, whereas the 95% CI

recreational runners contained a zero-value in a smaller percentage of the GCT located only in the middle of the GCT at the curve peak height. The results of this study suggest that interchangeability between shank-mounted IMUs and force plates may be very limited when estimating temporal gait events and kinetics. While agreement was low between F-t curves after the peak in skilled runners, use of shank-mounted IMUs to estimate F-t curves may have several benefits still in skilled runners when assessing peak forces and force development from initial contact until peak force.

ACKNOWLEDGMENTS

I am extremely grateful for everyone that has played a part in my journey to reach my goals both in my education and in the professional world. To my parents, Dave and Para, none of this would have even been possible without your love and support. You both have supported and loved me unconditionally throughout my entire educational career, and I cannot thank you both enough for the help yall constantly gave. To my two brothers, Deylan and Tanner, both of you have constantly challenged me throughout my life to and to not give up on the dreams I pursued on this path.

To my professors, past and current, thank you for the knowledge that you passed down to me during my education. To Dr. Bosak, thank you for challenging me not only in the classroom, but in my life as well. You planted the seed that made me want to pursue this career goal and pushed and prepared me to continue along with the process, no matter how difficult it was at times.

To my Committee, Dr. Michael Stone, Dr. Satoshi Mizuguchi, Dr. Matt Sams, and Dr. Brad DeWeese, thank you for your help and encouragement during this process. I am beyond grateful for the knowledge that was passed onto me, as well as the patience that each one of you had with me during the times when this project presented difficult struggles to overcome.

To my mentors, Dr. Brad DeWeese and Coach Meg Stone, I have no words to express my gratitude towards you both. Your passion for sport and desire to grow leaders in sport can never be overlooked. The incredible opportunities that I was given because of you two have left me humbled and make me aim to become more like you both when the opportunity comes for me to mentor someone.

To my friends and fellow classmates that shared this journey with me, I could not have done without everyone's support.

Lastly, to my wife, Kristen, thank you for your constant love and support. You have been by my side through all of this, and I am grateful for your constant encouragement during this tough part of my career.

TABLE OF CONTENTS

LIST OF TABLES

LIST OF FIGURES

Chapter 1. Introduction

Running kinetics and temporal gait events are important variables to consider when monitoring runners. Knowledge of these variables has opened the doors for understanding different aspects of sport performance and how factors such as fatigue and adaptations to different training stimuli affect performance. Temporal gait events like ground contact time (GCT), flight time (FT), and step kinetics/peak force (PF) are a few variables that have been linked to improved running economy, which has been defined as a major component differentiating success in elite level runners (Giovanelli et al., 2017; Mikkola et al., 2016; Milbrath et al., 2016; Saunders et al., 2004). The gold standard methods for measuring these variables during running are embedded or treadmill-equipped force plates and motion capture systems. While very accurate, they have the downside of being costly and limited to use in a laboratory setting.

Force-time curve models have allowed for visualization of force application during different movements, such as running and sprinting (Blickhan, 1989; Clark et al., 2014; Clark et al., 2017). The first model developed was the Spring-Mass Model (SMM) (Blickhan, 1989). This model describes the body as a massless spring that compresses at touchdown, stores elastic energy, and releases that energy during the propulsion phase (Alexander, 1992; Cavagna et al., 1964; McMahon & Chang, 1990). While this model was accurate when modeling forces during hopping and slow velocity running, the three assumptions of the simple-stance SMM were not valid for high velocity running and sprinting and resulted in low accuracy when modeling force-time curves. Goodness-of-fit tests showed that sprinters running at high speeds demonstrated asymmetrical force-time curves compared to those predicted by the SMM ($R^2 = 0.782 \pm 0.016$) (Clark et al., 2014). The Two-Mass Model, which breaks the body into two separate masses, was

introduced as a potentially more accurate method of modeling runners and sprinters "force-time characteristics" (Clark et al., 2017). Initial research on the TMM successfully predicted force-time curves from not only slow and fast running velocities, but also for athletes demonstrating both fore-foot and rear-foot strike patterns.

With their small size, low cost, and non-invasive use during research and monitoring, IMUs have allowed for higher ecological validity during athlete monitoring. Inertial measurement units contain triaxial accelerometers, gyroscopes, and magnetometers (Al-Amri et al., 2018), which allow for a more complete motion analysis during human movements such as running and sprinting. When compared to gold standard reference systems (force plates, motion capture systems), variables such as GCT ($r \geq 0.99$), PF ($r \geq 0.88$), and angular velocity ($r > 0.99$), have demonstrated acceptable validity when estimated from IMU data (Channells et al., 2006; Macadam et al., 2019; Purcell et al., 2006; Setuian et al., 2018). Various models to estimate running variables from IMU data have been shown to have discrepancies (Kenneally-Dabrowski et al., 2017; Macadam et al., 2019; Setuian et al., 2018). However, two conditions that have been consistently related to higher or lower validity scores are the placement of the sensors on the body and the capture frequency of the sensors. For example, Kenneally-Dabrowski and colleagues (2017) demonstrated units sampling under 200 Hz that were placed further from the segment of interest demonstrated poor validity ($r = 0.088$) in comparison to force plates. Thus, IMUs placed closer to the source of impact and sampling at sufficiently high frequencies may improve the validity of data recorded during running and sprint monitoring.

Therefore, the purpose of this dissertation is two-fold. The first purpose is to validate the measurement of temporal gait events and step kinetics such as GCT, FT, ST, and ground reaction forces estimated from shank-mounted inertial measurement units (IMU, Blue Thunder, Vicon) in

comparison to data derived from a force plate-equipped treadmill. The second purpose of this study is to validate the calculation of force-time curve shapes derived from the integration of shank-mounted IMU data and the TMM.

Chapter 2. Comprehensive Review of Literature

Running Performance Variables and Metrics

Advancements in running and sprint performance have developed from the knowledge gained through studies concerned with the different aspects that relate to elite-level running. In elite-level sport, the small advantages an athlete has over competitors can be the deciding factors between winning and losing. One of the primary influences related to elite running outcomes is running economy. Running economy is the energy (i.e., oxygen consumption) required to maintain a submaximal velocity (Daniels, 1985). In runners with similar maximal oxygen consumption profiles, the athletes who have the ability to sustain the lowest metabolic cost at the same submaximal paces are generally the athletes who come out on top. One of the issues with determining running economy is that it requires expensive pieces of equipment (e.g. metabolic carts) that generally restrict measurements to a laboratory setting. Due to the invasiveness and poor ecological validity of lab-based physiological and biomechanical testing, recent research has aimed to approximate running economy through running efficiency-related measures (Hunter et al., 2015; Saunders et al., 2004; Williams et al., 1987).

Running efficiency is determined by the ratio between the mechanical energy produced during exercise and the energy cost of the exercise. Biomechanical factors and gait temporal events seem to be two of the most influential components for increasing running efficiency (Milbrath et al., 2016). When assessing efficiency in elite-level running and sprinting, standard variables include GCT, ankle/leg stiffness and vertical oscillation. The ability to measure these variables has led to further knowledge of what training types lead to either improvements of decrements in these variables (Dumke et al., 2010; Giovanelli et al., 2017; Mikkola et al., 2011).

Ground Contact Time

Extensive debate surrounds the importance of short GCT on running economy (Di Michele & Merni, 2014; Folland et al., 2017; Nummela et al., 2007; Santos-Concejero et al., 2014). While Di Michele and colleagues (2014) showed poorer running economy from shorter GCT, a potential explanation for this result could be the study's small sample size of relatively weak runners. Research on stronger, faster, and overall more skilled runners and sprinters show these athletes have the ability to produce most of the ground reaction forces during the early stages of the contact phase (Clark et al., 2017; Weyand et al., 2010; Weyand et al., 2012). Therefore, while shorter GCT can potentially lead to either improved or impaired running economy, the deciding element seems to be the ability or inability for that runner to produce high forces quickly. The goals of this approach to force development are two-fold: 1) reduce the athlete's braking time and 2) minimize neuromuscular activation and resultant energy cost during GCT (Barnes & Kilding, 2015; Miller et al., 2012; Nummela et al., 2008; Paavolainen et al., 1999).

Vertical Oscillation

In running, vertical oscillation (VO) refers to the movement/displacement of the COM in the vertical direction. Typically, lower VO has been associated with enhanced running economy (Cavagna et al., 1997; Cavagna et al., 2005; Svedenhag & Sjodin, 1984; Tartaruga et al., 2012). This finding is further supported by recent research demonstrating a strong relationship between pelvic VO, greater energy cost, and decreased performance in running ($r = 0.534$, $P < 0.001$) (Folland et al., 2017; Halveron et al., 2015). The energy cost related to the degree of change in VO is directly proportionate to the amount of work required to propel the body forward due to

the force from gravity. That is, the higher the VO, the more work required to overcome the force due to gravity (Folland et al., 2017; Kobsar et al., 2019; Slawinski & Billat, 2004). Biomechanical factors that assist with reducing VO are greater stiffness of the lower leg and ankle. Greater stiffness in the lower extremities allows for reduced time to stabilize and reduces aberrant limb movement (collapse) during contact (Gunther & Blickhan, 2002).

Ankle/Leg Stiffness

Shorter GCT, greater muscle pre-activation, and enhanced ability to produce high forces quickly are three factors that can positively influence an athlete's lower-leg stiffness (Dalleau et al., 1998; Paavolainen et al., Nummela et al., 2008; 1999). Enhanced lower leg stiffness has been correlated to higher running economy in various subject groups (Arampatzis et al., 2006; Dalleau et al., 1998; Franklin et al., 2003). Findings that support this observation are the ability of runners with greater lower leg stiffness to transition to the propulsion phase from the braking phase more quickly and overall enhanced motor unit recruitment in pre-activation muscle activity (Avela & Komi, 1998; Heise et al., 2008). Finally, increased muscle-tendon stiffness has been shown to be more efficient with higher energy storage and release during the stretch-shortening cycle (SSC) (Albracht & Arampatzis, 2013).

Running Force Modeling Applications

Spring-Mass Model

The ability to gather force-time data for running/sprint steps has led to great advancements in sport performance. This concept was first explored with the SMM (Blickhan, 1989). The SMM describes the body as a simple massless spring that compresses at touchdown,

storing energy to be released during take-off (*Figure 1*) (Alexander, 1992; Blickhan, 1989; Cavagna et al., 1964; McMahon & Cheng, 1990).

Figure 2.1.

The Simple Stance Mass Model (Blickhan, 1989).

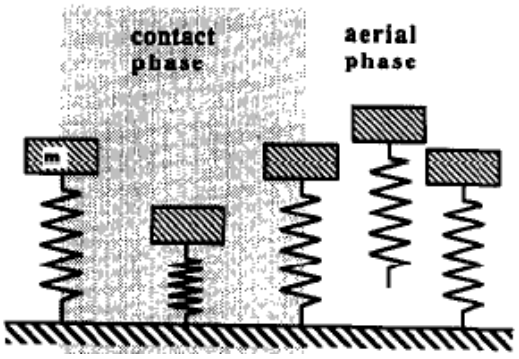

The stretch-shortening cycle (SSC) is the concept most responsible for how the SMM functions (Blickhan, 1989; Dickinson et al., 2000; Farley et al., 1993; Komi, 1984). At each initial foot contact, the force of gravity causes the lower limb to compress, which causes the storage of elastic energy. As the contact leg goes from mid-stance to take-off, the stored energy is released (Dalleau et al., 1998; Farley et al., 1991; Farley & Gonzalez, 1996; Ferris et al., 1998). One of the key factors that determines the effectiveness of the SMM is vertical stiffness (Brughelli and Cronin, 2007; Farley & Gonzalez, 1996; Girard et al., 2011; Morin et al., 2005). The greater the vertical stiffness, the higher the maximum velocity and force that can be attained (He et al., 1991; McMahaon et al., 1987).

Two-Mass Model

One limitation of the simple SMM was that the calculated force-time curves were not sufficiently accurate to be representative of the force-time curves of skilled runner and sprinters at high speeds, demonstrating mean R^2 values of 0.782 ± 0.016 (Clark, 2014). As shown in previous research, this limitation can be traced to only using slower speeds and hopping when comparing curves between several movement conditions in most studies (Bruggeman et al., 2009; Farley & Gonzalez, 1996; Farley et al., 1998; McMahon & Cheng, 1990; Srinivasan & Holmes, 2008). The SMM's demonstrated weaknesses in force-time calculations of faster/more skilled sprinters originates from several simplifications in the model calculations. The first simplification of the SMM is that the shape of the force-time curve is always a half-sine (*Figure 2.2)*.

Figure 2.2.

Half-sine SMM Force-Time Curve (Clark et al., 2014)

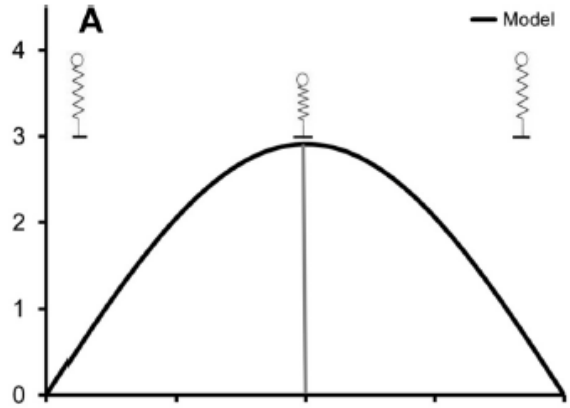

While trying to differentiate between the force-time curves between slow vs. fast runners, each group demonstrates having similar characteristics of lower limb patterns during flight

(Weyand et al., 2000; Weyand et al., 2010). Therefore, the differences lay in the ability of the more skilled/faster sprinters to produce more force in less time during foot contact, with the resultant waveforms from faster speeds presenting a more asymmetrical pattern.

The second simplification of the SMM is that the displacement of the center of mass (COM) is even throughout the entire foot contact phase. Finally, the model assumes that peak vertical force always occurs in the middle of the ground contact phase, which coincides with the COM's lowest point. While the SMM's predictions proved fairly accurate at slow to moderate speeds, force-time curves from faster runners and sprinters consistently demonstrated asymmetrical patterns, with the highest forces achieved prior mid-stance (Blickhan, 1989; Bundle & Weyand, 2012; Weyand et al., 2009; Weyand et al., 2010). In addition to the SMM's inaccuracies in modeling F-t curves at high speeds, difficulties also arise in modeling fore-foot strikes (Ly et al., 2010; Zadpoor and Nikooyan, 2010) and the falling edge of the F-t curve (Clark et al., 2014).

Other approaches to predict waveforms have been proposed that account for the limitations of the SMM. One such model that was successful in predicting waveforms developed by Bobbert and colleagues (1991) used a seven-component acceleration model. The seven rigid bodies in this model were comprised of both feet, both shanks, both thighs, and a combined segment of the trunk, arms, and head. While successful in predicting the waveforms, utilization of seven different body segments proved to not be very practical. As a simplification to the seven mass system, Clark and colleagues (2014) proposed an alternative model consisting of two body masses (two-mass model, TMM) in which the first mass represents the shank of the contact leg (~8% body mass) and the second mass represents the remainder of the body (Clark et al., 2014). Each mass, when coupled with three step-related temporal events and kinetic components, allows

for the calculation to two separate vertical impulses that can be summed together to produce a single force-time waveform (*Figure 3*).

Figure 2.3.

The TMM Force-Time Curve (Clark et al., 2017). Impulse 1 (red) represents the force of the first mass (shank) and Impulse 2 (green) represents the force of the second mass (body). The impulses are summed to give the total impulse curve (Blue).

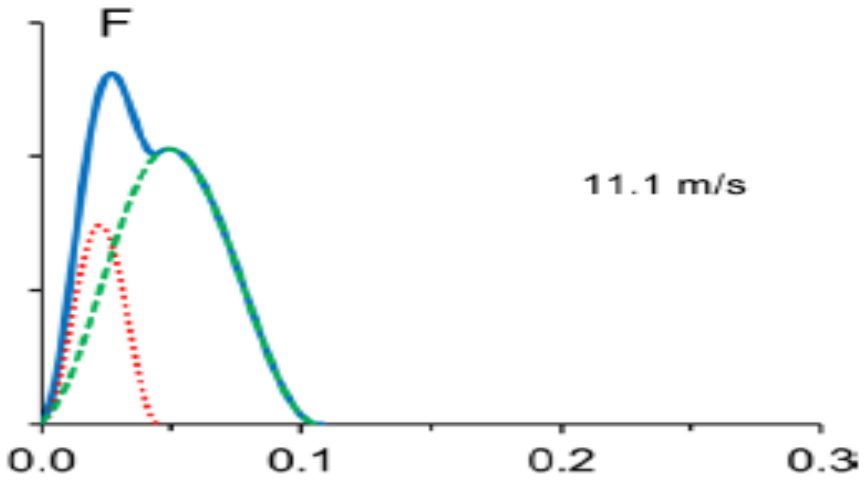

These three additional components are the GCT, aerial time (FT), and lower-limb acceleration data of each step (Clark et al., 2017). The resultant equation for calculating total impulse is:

EQUATION 1: Calculation of Total Impulse

$$J_T = J_1 + J_2 = F_{Tavg} t_c$$

Where J_T is the combined impulse from J_1 (impulse 1) and J_2 (impulse 2), F_{Tavg} is the average vertical ground reaction force, and t_c is the ground contact time. The average force may be calculated as follows:

EQUATION 2: Calculation of Average Vertical Ground Reaction Force during GCT

$$F_{Tavg} = mg\ ((t_c + t_a)/(t_c))$$

The total body mass is represented by m, acceleration from gravity ($9.81 m*s^{-2}$) is g, and t_c and t_a are contact time and aerial time of each step. Impulse 1 can be calculated through the following:

EQUATION 3: Calculation of Mass 1 Impulse

$$J_1 = F_{1avg}(2\Delta t_1) = (m_1(\Delta v_1/\Delta t_1) + m_1 g)(2\Delta t_1)$$

Where F_{1avg} is the average force of the first mass from initial contact until shank stabilization, Δt_1 is the time from initial touchdown until zero velocity/stabilization, m_1 is the mass of the shank (8% of total body mass, and Δv_1 is the change of velocity of the first mass during the time until stabilization, (Clark et al., 2017). Finally, Impulse 2 is calculated by the following equation:

EQUATION 4: Calculation of Mass 2 Impulse

$$J_2 = F_{2avg}\ t_c = J_T - J_1$$

Where F_{2avg} is the average force of the second mass' impulse during ground contact time (Clark et al., 2017). In place of the half-cosine functions, Clark and colleagues (2017) demonstrated a raised bell function more accurately represented the two impulses and final resultant impulse. Similar to the SMM, the TMM was able to accurately estimate force-time data for rear-foot strikers and slower speed running. Unlike the SMM, however, the TMM also accurately estimated kinetic data for forefoot strikers and faster runners.

Accelerometry: Inertial Sensors, Applications, and Limitations

Accelerometers/Inertial Sensors

Research involving accelerometers and similar technologies has historically focused on robotics and military application; however, the development of smaller integrated units (micro-electrical-mechanical systems, MEMS) has led to an increase of research in human applications

(Passaro et al., 2017; Pirinen et al., 2020; Tobin et al., 2020). Uses of accelerometers and inertial sensors with human research have involved multiple conditions such as healthy and unhealthy populations (Klucken et al., 2013; Zago et al., 2018). These small units have assisted with gaining a greater understanding of how different diseases can affect day-to-day living in individuals such as gait parameters in patients with Parkinson's disease.

Inertial measurement units (IMUs) are MEMS that generally contain multi-axis accelerometers, gyroscopes, and magnetometers (Al-Amri et al., 2018). Accelerometers are devices that measure acceleration, or the rate of change of velocity. Accelerometers typically are tri-axial and measure the rate of change in velocity in the three different planes of movement (anterior-posterior, lateral, vertical) (Schutz et al., 2001). Accuracy of the raw data from accelerometers in human research is typically dependent on four factors: the activity being performed, the posture/orientation of the subject, the position/location of the sensor on the body, and the orientation of the sensor at the placed location (Mathie et al., 2004). One of the major disadvantages of using only an accelerometer is that these devices only measure the change in velocity in a linear plane. To overcome that limitation of accelerometers, IMUs are generally equipped with a gyroscope and sometimes magnetometer. Gyroscopes are devices that allow the measurement of angular velocity, or the rate of rotation around a particular axis (Passaro et al., 2017). A gyroscope operates by a spinning mass that rotates around one of three axes, installed on gimbals that allow for free rotation. The direction in which the mass spins is related to the reference inertia, under the condition that a constant torque is applied to the mass (Passaro et al., 2017). Magnetometers are devices that are sensitive to the strength and direction of a magnetic field. They assist with determining the orientation of a body, as well as assist with drift-correction from the gyroscope (Wittman et al., 2019). Thus when properly instrumented, IMUs

are able to capture 3-dimensional movement and have allowed for more advanced total body motion analysis

Validity and Reliability in Running Metrics

Due to IMUs' small size, low cost, and potential for high ecological validity, a number of studies have aimed to quantify their reliability and validity in measuring running performance metrics (Al-Amri et al., 2018; Robert-Lachaine et al., 2017). These validation and reliability studies have examined a range of conditions to determine their impact on the validity and reliability of wearable IMUs.

Temporal Measures and Gait Events. The highest validity of recording gait events/temporal measurements has been observed when the inertial sensors are placed on the lower limbs or the lumbar spine (Schmidt et al., 2016; Ammann et al., 2016; Bergamini et al., 2012; Kenneally-Dabrowski et al., 2017; Purcell et al., 2006). This observation has held true across a variety of "gold standard" reference systems, including force plates, high-speed cameras, and photoelectric systems. Despite generally strong relationships, not all research has demonstrated agreement between the reference system and IMU. For example, Kenneally-Dabrowski and colleagues (2017) found low validity ($r = -0.177$) in IMU in reference to embedded force plates. The researchers, however, placed the IMUs between the scapulae, which could have distorted the acceleration measurements during each step (Macadam et al., 2019). Compounding the problem of unit placement is the sampling rate of the IMUs. Researchers have typically found the sampling frequency should be in excess of 200 Hz, with higher frequencies improving the unit's measurement validity (Ammann et al., 2016). Taken together, wearable

IMUs should be placed on or near the lower limbs and should sample in excess of 200 Hz when the goal is to measure temporal gait events such as contact time and aerial time.

Forces. Placement of inertial sensors closest to the COM (Lumbar and Sacrum) resulted in the highest levels of validity of vertical and horizontal force ($r \geq 0.88$) as well as resultant peak forces ($r \geq 0.76$) (Gurchiek et al., 2017; Setuian et al., 2018). Similar to measuring GCT, the further away from the COM the sensor was placed (e.g., T2 spine), the less valid and more varying the results were when measuring forces from running steps (Wundersitz et al., 2013). Thus, we can theorize that the further an inertial unit is away from the point of ground contact (the foot), the lower the measurement validity. Similar to temporal gait events, sampling frequencies in excess of 200 Hz have been demonstrated to have higher measurement validity for peak vertical force (Macadam et al., 2019).

Sensor Displacement and Angular Velocity. High levels of validity with angular displacement of the trunk ($r \geq 0.99$) and shank angular velocity/acceleration (RMSE < 10%) were reported when placement of the units was closest to the body segment interest in reference to high-speed cameras (Bergamini et al., 2013; Channells et al., 2006). Similar to force and temporal data, IMU estimation of displacement and angular velocity suffers as the unit moves further away from the area of interest. For example, Kenneally-Dabrowski and colleagues (2017) observed low levels of validity for medial-lateral axis step displacement ($r = 0.088$) with inertial senor placement between the scapulae in reference to force plates. Conversely, Bergamini and colleagues (2013) observed high validity ($r = 0.998$) for trunk angular displacement with inertial sensors placed on the lumbar spine in reference to high-speed cameras.

Summary

To account for the limitations of the SMM to predict waveforms for running steps, the Two-mass model was developed. The TMM successfully estimated force-time curves for running steps not only for fore-foot and rear-foot strikers, but also for both slower and faster running speeds. Several components needed to model the waveforms are temporal gait events that have been linked to increased running economy in elite runners. Use of inertial sensors has grown rapidly in research because of their small size, low cost, and potential for high ecological validity. A range of conditions has been analyzed to determine the validity of IMUs and their ability to estimate running performance measurements. When coupled together, sampling frequencies of at least 200 HZ and sensor placement closest to the body segment of interest have demonstrated the highest validity. Reliability and validity measurements for temporal events and kinetics have demonstrated varying results based on placement of the sensor and the "gold standard" reference system utilized during the comparison. When running performance measurements such as temporal gait events and kinetics are of interest, inertial placement on or close to the lower limbs and sample rates of at least 200 Hz has demonstrated the highest validity.

Chapter 3. Agreement of Temporal Gait Events and Kinetics Derived from Shank-Mounted Inertial Measurement Units

AUTHOR: Smith, Austin[1]; Sams, Matt[2]; Mizuguchi, Satoshi[1]; DeWeese, Brad[1]; Stone, Michael[1]

AUTHOR AFFILIATIONS:

[1] Center of Excellence for Sport Science and Coach Education, Department of Sport, Exercise, Recreation and Kinesiology, East Tennessee State University, Johnson City, TN, USA

[2] Performance Science, Kansas City Royals, Surprise, AZ, USA

CORRESPONDING AUTHOR:

Austin P. Smith

East Tennessee State University

Department of Sport, Exercise, Recreation, and Kinesiology

Johnson City, TN, 37601

Phone: 804-525-8379

smithap4@etsu.edu

Agreement of Temporal Gait Events and Kinetics Derived from Shank-Mounted Inertial Measurement Units

Abstract

Inertial measurement units (IMUs) and other small wearable sensors have been useful tools in sport monitoring and research due to their low cost and non-invasive capabilities. Body placement closest to the point of impact and higher sampling frequencies have resulted in higher validity for recording variables during running from several different accelerometers and inertial sensors. The purpose of this study was to assess the validity of running temporal gait events and kinetics derived from commercial-based shank-mounted IMUs in reference to a force plate-equipped treadmill. Ten subjects completed submaximal treadmill tests with speeds ranging from 8mph to 15mph. Raw data from the IMUs were filtered and plotted to manually determine ground contact time (GCT), flight time (FT), and total step time (ST). Peak force was estimated from the acceleration data from each shank via the proposed equations of the two-mass model. No statistically significant differences existed between the variables calculated from the IMUs and the treadmill force plate ($p > 0.05$) and moderate to very large relationships ($r = 0.771 – 0.998$) existed among variables over the averages of each speed. When assessing individual steps, no statistically significant differences ($p > 0.05$) were present between GCT, FT, and PF paired with mostly moderate to very large relationships at every speed. No statistically significant differences were present with ST based on the robust t test. This evidence suggests that shank-mounted IMUs are potential substitutes for force plates for

measuring temporal gait events and peak forces during upright running across multiple speeds.

Keywords: Inertial Measurement Unit, Temporal Gait Events, Peak Force, Running

Introduction

Knowledge of temporal gait events and kinetics have led to increased understanding of walking, running, and sprinting and their impact of overall health and sport performance. For sport performance, the ability to analyze variables such as ground contact time (GCT), flight time (FT), and peak force (PF) during running has allowed for athlete monitoring to become more efficient in running-based athletes. These have led to investigations regarding two aspects of sport, 1) how to alter the variables through different training types and modalities and 2) how alterations in these variables impact overall running performance (Dumke et al., 2010; Giovanelli et al., 2017; Mikkola et al., 2011). Currently the most widely accepted methods for measuring these variables are force plates and motion analysis camera systems. However, these methods are restricted in their ecological validity because they are not only expensive, but also generally limited to a laboratory setting.

While historically used during robotics and military use, smaller, commercialized inertial measurement units (IMUs) have become available for use in human research (Al-Amri et al., 2018; Klucken et al., 2013; Robert-Lachaine et al., 2017; Zago et al., 2018). IMUs consist of multi-axis accelerometers, gyroscopes, and magnetometers that assist with measurement of total-body motion. When compared to gold standard reference methods (e.g., force plates, motion capture systems), running temporal gait events such as ground contact time ($r \geq 0.99$), CV < 4%,

ICC $\geq$ 0.91), and step time (LoA bias 25ms) and running kinetics such as peak forces (r $\geq$ 0.88, ICC $\geq$ 0.88) calculated from IMUs were reported to have good validity and reliability (Ammann et al., 2016; Gurchiek et al., 2017; Macadam et al., 2019; Purcell et al., 2006; Schmidt et al., 2016; Setuain et al., 2018). Several conditions have been suggested in order to achieve the highest validity. First, a minimum recording frequency of at least 200Hz. Second, the placement of the sensors has been found to produce higher validity measurements when placed closer to the area of interest, such as the lower legs for running metrics (Purcell et al., 2006; Schmidt et al., 2016). The benefits of using IMUs in measuring running performance have led to more ecological validity. However, measurement validity varies among different brands of IMUs. Therefore, the purpose of this study is to assess the agreement of an IMU (Blue Thunder Inertial Measurement Units, Vicon) for the measurement of running temporal gait events such as GCT, FT, and ST and running peak forces in reference to treadmill equipped force plates.

Methods

Subjects

Ten runners volunteered to participate in the study (5 male, 5 female, 24.5 ± 3.6 yrs, 63.2 ± 9.46 kg). Each subject had been actively running for at least 1 year, with past competition experience preferred. Further breakdown of the group showed subjects consisting of four recreationally trained subjects and six skilled runners (1 Olympian and 5 collegiate). Furthermore, subjects did not have any musculoskeletal injuries within the past 6 months, or any other current condition that could potentially lead to complications during exercise. All subjects read and signed an informed consent document prior to participation in the study, as approved by the university's Institutional Review Board.

Experimental Design

Each subject underwent one testing session in the laboratory. Subjects were first assessed for body mass measurements using a standard scale. Each subject was then prepared to run a discontinuous graded treadmill test. Blue Thunder Inertial Measurement Units (Vicon Motion Systems, United Kingdom) were placed immediately superior to the medial malleolus on both shanks. Recording frequency for the IMUs was 500Hz, with data collection accomplished through a smartphone application (IMU Research 3.1, Vicon). The treadmill was a high-speed treadmill that was equipped with a force plate. Sampling rate of the force plate was 1000 Hz, and data was recorded and processed in LabVIEW. Treadmill tests consisted of speeds 8mph-15mph, with each stage lasting 20-40 seconds. Rest time between each stage lasted a minimum of 60 seconds, to ensure the least amount of fatigue was accumulated during the faster speeds.

Signal Processing

Inertial measurement data were filtered through a second order band-pass Butterworth filter (0.7Hz to 50Hz) (Charry et al., 2009a; Charry et al., 2009b; Lai et al., 2008). Following the filtering, the y-axis acceleration data, z-axis gyroscope data, and the resultant acceleration data were plotted to manually identify specific gait events. The resultant acceleration was calculated from taking the square root of the sum of squares of the ‘x’, ‘y’, and ‘z’-axis acceleration data. Ground Contact (GC) and time to zero acceleration (T_0) were defined by the onset and termination, respectively, of the first rise in the y acceleration data, located in between two gyroscope peaks (Figure 4). Toe Off (TO) was represented as the first spike in the resultant acceleration data immediately after the highest gyroscope spike situated between the two gyroscope peaks (Figure 4).

Figure 3.1.

Location of key timepoints to calculate three temporospatial gait characteristics.

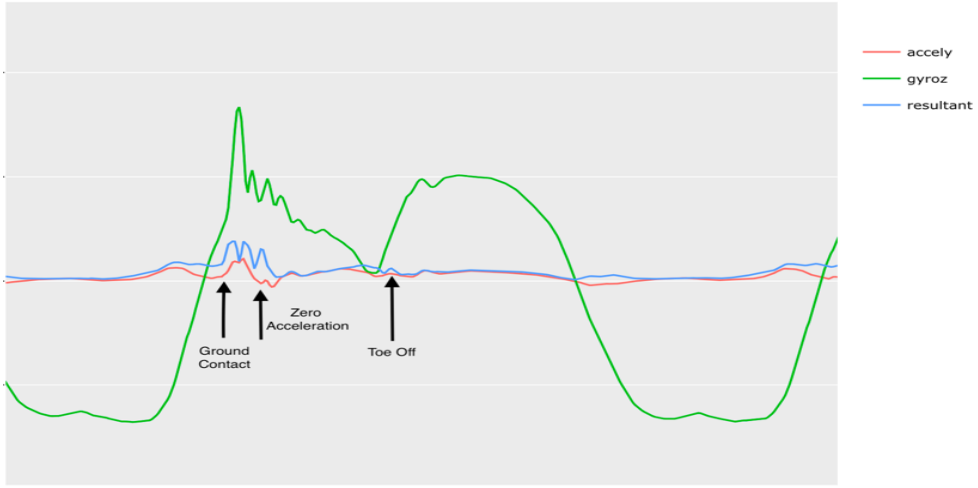

The timepoints for initial contact, time until zero acceleration, and toe off allowed for the calculation of Ground Contact Time (GCT), Time to shank stabilization (TSS), Flight Time (FT), and total Step Time (ST). Utilizing the manually determined timepoints and acceleration data, Impulse 1 and Impulse 2 were calculated using the equations developed by Clark and colleagues (2017). Total impulse was then calculated by adding Impulse 1 and Impulse 2 together. Peak Force (PF) was acquired after the total impulse/impulse curve was developed for each step. Raw data from the treadmill force plate were collected via a custom program (LabVIEW 2018, National Instruments) and exported for processing and analysis. The first six steps of every speed were omitted from the analysis to allow for gait stabilization.

Statistical Analysis

All data processing and statistical analysis were performed with the statistical software R (version 3.0.1+) (R Core Team, 2019). Two different conditions were assessed for agreement

between the IMU and treadmill derived variables, 1) individual step comparison with randomly selected steps from each speed, and 2) averages of 20 randomly selected steps from every speed. Paired-sample t-tests were performed to determine if statistically significant differences existed between the force plate and IMU variables. Pearson's correlations were used to evaluate relationships between the two devices. Correlations were rated as trivial (0-0.10), small (0.11-0.39), moderate (0.40-0.69), large (0.70-0.89), and nearly perfect (0.90-1.00) (Mukaka, 2012). Lastly, Hedge's *g* effect sizes were calculated to describe the magnitude of difference between devices. Magnitudes thresholds of effect sizes were interpreted as 0-0.2, 0.21-0.6, 0.61-1.21, 1.21-2.0, and 2.0 and above as trivial, small, moderate, large, and very large (Hopkins, Batterham, Marshall, & Hanin, 2009). The critical alpha was set at 0.05. The assumptions of general linear model were assessed for each model. Shapiro-Wilks test was performed to assess the distribution of residuals. Independence of error was assessed with Durbin-Watson's test. Lastly residuals were plotted against fitted values to assess for heteroscedasticity. For all violations except for independence of error, robust alternatives were used (Mair & Wilcox, 2020). Force plate and IMU data were reported as mean ± SD, whereas correlation coefficient and effect sizes are presented as the respective point estimate.

Results

Gait Event and Kinetic Averages

No assumptions were violated with peak force, ground contact time, and flight time. Step time residuals violated normality distributions based on Shapiro-Wilks t-tests ($p < 0.05$). When steps were averaged over a given speed, no statistically significant differences were observed between the force plate and IMU for GCT ($p > 0.05$, $-0.051 < g < 0.049$), FT ($p > 0.05$, $-0.051 <$

$g < 0.049$), ST ($p > 0.05$, $-0.051 < g < 0.049$), and PF ($p > 0.05$, $-0.051 < g < 0.049$) (**Tables 3.1-3.3**). Correlations between devices ranged from very large (GCT, $0.771 < r$ 0.89) to nearly perfect (FT, $0.904 < r < 0.988$; ST, $0.964 < r < 0.998$; PF, $0.971 < r < 0.993$).

Table 3.1.

Average Ground Contact Time per Speed

Speed	Force Plate	IMU	Pearson's	Hedge's *g*
8	212.57 ± 12.83	211.99 ± 8.2	0.890	0.005
9	199.3 ± 12.07	199.66 ± 12.07	0.825	0.046
10	187.47 ± 9.29	186.05 ± 6.35	0.787	-0.048
11	176.24 ± 8.88	175.49 ± 6.16	0.771	-0.016
12	164.63 ± 7.83	164.4 ± 5.27	0.798	-0.004
13	155.98 ± 8.42	154.87 ± 5.51	0.844	0.009
14	149.46 ± 8.88	147.84 ± 4.98	0.870	-0.019
15	142.57 ± 8.23	141.07 ± 6.21	0.881	-0.019

Data presented as mean ± SD in milliseconds. Correlation coefficients and effect sizes presented as point estimates.

Table 3.2.

Average Flight Time per Speed

Speed	Force Plate	IMU	Pearson's	Hedge's *g*
8	120.42 ± 15.24	120.35 ± 12.61	0.964	0.005
9	125.29 ± 13.21	124.67 ± 10.4	0.904	0.046
10	128.6 ± 12.67	129.15 ± 13.81	0.959	-0.048
11	129.33 ± 11.98	129.45 ± 11.12	0.966	-0.009
12	128.68 ± 11.66	128.73 ± 13.12	0.951	-0.004
13	126.93 ± 13.9	126.83 ± 13.61	0.970	0.008
14	121.32 ± 19.99	121.81 ± 18.04	0.988	-0.022
15	117.23 ± 19.11	117.59 ± 18.8	0.988	-0.019

Data presented as mean ± SD in milliseconds (ms). Correlation coefficients and effect sizes presented as point estimates.

Table 3.3.

Average Peak Force per Speed

Speed	Force Plate	IMU	Pearson's	Hedge's *g*
8	1730.39 ± 316.92	1697.1 ± 286.41	0.990	0.005
9	1763.26 ± 319.07	1756.36 ± 289.22	0.993	0.046
10	1806.32 ± 310.68	1832.36 ± 298.92	0.991	-0.048
11	1836.91 ± 306.7	1876.25 ± 281.71	0.990	-0.016
12	1862.68 ± 311.2	1919.85 ± 272.21	0.982	-0.004
13	1883.23 ± 332.09	1956.29 ± 294.93	0.992	0.009
14	1905.34 ± 320.02	1960.65 ± 294.86	0.977	-0.022
15	1936.68 ± 318.02	1971.68 ± 300.09	0.971	-0.019

Data presented as mean ± SD in Newtons (N). Correlation coefficients and effect sizes presented as point estimates.

Robust alternatives for paired-sample t-tests and effect sizes for ST demonstrated no statistically significant differences between devices ($p > 0.05$, $0.00 > ES > 0.07$) (**Table 3.4**) and robust correlations ranged from large (8mph, $r = 0.785$) to nearly perfect (9-15mph, $0.943 > r > 0.999$).

Table 3.4.

Robust Alternatives for Average Step Time per Speed

Speed	Force Plate	IMU	Trimmed Mean Diff	Correlation	Effect Size
8	332.99 ± 12.76	332.35 ± 11.78	1.075	0.785	0.09
9	324.59 ± 13.73	324.59 ± 12.51	0.361	0.976	0.028
10	316.07 ± 14.64	315.2 ± 15.68	0.535	0.943	0.066
11	305.57 ± 15.96	304.94 ± 14.43	0.063	0.989	0.00
12	293.31 ± 15.37	293.13 ± 15.22	-0.011	0.999	0.00
13	282.91 ± 18.39	281.69 ± 15.98	-0.036	0.999	0.00
14	270.78 ± 20.62	269.65 ± 18.09	0.279	0.999	0.009
15	259.8 ± 21.98	258.67 ± 19.77	0.324	0.999	0.009

Data presented as mean ± SD in milliseconds (ms). Correlation coefficients and effect sizes presented as point estimates

Selected Step Comparison

No assumptions were violated for peak force, ground contact time, and flight time. Step time residuals violated normality distributions based on Shapiro-Wilks t-tests ($p < 0.05$). No statistically significant differences were found between the two devices for GCT ($p = 0.316 – 0.985$; $0.02 < g < 0.361$), FT ($p = 0.148 – 0.719$; $0.02 < g < 0.36$), or PF ($p = 0.174 – 0.923$; $0.02 < g < 0.361$) (**Table 3.5-3.7**).

Table 3.5.

Ground Contact Time for Selected Steps per Speed

Speed, Step #	Force Plate	IMU	Pearson's	Hedge's *g*
8mph				
8	210.14 ± 16.56	209.8 ± 10.31	0.937	0.019
14	211.59 ± 14.66	214.8 ± 8.78	0.799	0.120
28	213.06 ± 13.7	213.01 ± 8.38	0.850	0.046
9mph				
10	201.27 ± 14.16	198.18 ± 10.03	0.762	0.253
12	199.04 ± 13.85	200.39 ± 8.6	0.787	0.028
27	198.56 ± 12.34	198.89 ± 8.81	0.797	0.342
10mph				
11	187.08 ± 7.62	187.24 ± 4.24	0.739	0.107
18	188.82 ± 11.25	185.16 ± 8.92	0.671	0.216
26	188.52 ± 10.34	187.76 ± 6.6	0.791	0.046
11mph				
14	177.34 ± 9.67	175.77 ± 4.89	0.698	0.161
20	179.38 ± 10.27	176.57 ± 5.65	0.665	0.002
23	175.21 ± 6.64	176.28 ± 6.31	0.726	0.104
12mph				
7	161.68 ± 8.26	164.47 ± 5.42	0.809	0.20
15	164.31 ± 11.1	164.47 ± 6.99	0.879	0.084
29	163.43 ± 6.84	164.67 ± 3.14	0.443	0.055
13mph				
11	158.47 ± 11.29	156.68 ± 4.25	0.297	0.171
15	161.2 ± 13.6	156.28 ± 2.65	0.108	0.31
25	154.67 ± 9.3	155.48 ± 5.15	0.825	0.283
14mph				
9	148.55 ± 8.13	149.29 ± 6.03	0.906	0.046
17	149.81 ± 9.89	147.49 ± 3.85	0.397	0.335
21	145.91 ± 7.14	149.49 ± 4.19	0.5	0.146
15mph				
7	138.22 ± 9.24	140.08 ± 6.77	0.573	0.055
13	145.52 ± 7.81	142.27 ± 4.51	0.689	0.163
28	143.76 ± 10.51	139.73 ± 5.33	0.375	0.148

Data presented as mean ± SD in milliseconds (ms). Correlation coefficients and effect sizes presented as point estimates.

Table 3.6.

Flight Time for Selected Steps per Speed

Speed, Step #	Force Plate	IMU	Pearson's	Hedge's *g*
8mph				
8	120.02 ± 14.69	119.66 ± 14.83	0.926	0.002
14	120.12 ± 18.27	117.84 ± 16.72	0.911	0.120
28	120.02 ± 15.44	120.82 ± 13.41	0.898	0.046
9mph				
10	122.21 ± 11.05	125.37 ± 12.2	0.846	0.253
12	127.85 ± 11.44	128.2 ± 8.16	0.773	0.028
27	129.84 ± 16.72	123.15 ± 13.38	0.741	0.342
10mph				
11	124.2 ± 12.1	122.85 ± 11.78	0.524	0.107
18	132.52 ± 12.32	136.12 ± 16.99	0.715	0.216
26	131.33 ± 5.62	130.74 ± 13.99	0.343	0.046
11mph				
14	131.12 ± 11.35	120.02 ± 12.93	0.719	0.161
20	129.13 ± 11.32	129.16 ± 12.55	0.699	0.002
23	124.36 ± 12.52	125.65 ± 10.54	0.475	0.104
12mph				
7	127.48 ± 10.03	129.76 ± 11.43	0.523	0.20
15	128.31 ± 11.97	127.17 ± 9.77	0.87	0.085
29	127.58 ± 10.48	128.25 ± 10.64	0.507	0.057
13mph				
11	123.67 ± 12.46	121.96 ± 9.86	0.701	0.171
15	122.41 ± 11.61	118.85 ± 9.57	0.725	0.309
25	126.63 ± 10.67	123.64 ± 9.15	0.674	0.283
14mph				
9	112.99 ± 22.1	111.89 ± 17.27	0.854	0.047
17	124.82 ± 15.44	119.55 ± 12.95	0.868	0.335
21	119.48 ± 16.71	116.98 ± 14.42	0.874	0.146
15mph				
7	109.72 ± 15.05	108.61 ± 17.69	0.828	0.057
13	120.92 ± 16.54	116.99 ± 22.61	0.907	0.163
28	118.92 ± 23.94	122.73 ± 17.3	0.876	0.148

Data presented as mean ± SD in milliseconds (ms). Correlation coefficients and effect sizes presented as point estimates.

Table 3.7.

Results for Peak Force Step Comparison

Speed, Step #	Force Plate	IMU	Pearson's	Hedge's *g*
8mph				
8	1709.28 ± 351.34	1697.34 + 314.58	0.981	0.019
14	1723.02 + 373.15	1677.1 + 318.7	0.991	0.120
28	1705.99 + 355.93	1703.16 + 311.7	0.972	0.046
9mph				
10	1742.3 + 341.31	1771.4 + 351.88	0.984	0.253
12	1752.31 + 352.85	1774.9 + 294.6	0.988	0.028
27	1775.85 + 356.38	1751.1 + 330.0	0.974	0.342
10mph				
11	1793.91 + 271.04	1781.26 + 286.71	0.927	0.107
18	1812.16 + 348.41	1890.1 + 354.88	0.973	0.216
26	1781.58 + 319.89	1836.61 + 283.9	0.961	0.046
11mph				
14	1843.86 + 336.99	1872.79 + 296.03	0.977	0.161
20	1816.89 + 333.66	1877.14 + 320.4	0.963	0.002
23	1835.06 + 300.47	1841.35 + 286.83	0.966	0.109
12mph				
7	1870.91 + 328.71	1919.98 + 244.82	0.936	0.20
15	1876.39 + 347.43	1909.66 + 287.26	0.968	0.085
29	1887.74 + 301.04	1913.80 + 269.4	0.949	0.056
13mph				
11	1891.42 + 338.71	1898.22 + 283.72	0.975	0.171
15	1863.44 + 321.23	1883.53 + 288.89	0.969	0.310
25	1919.5 + 375.85	1933.21 + 309.05	0.984	0.283
14mph				
9	1895.68 + 345.18	1867.47 + 302.51	0.895	0.047
17	1944.12 + 350.75	1943.44 + 315.3	0.958	0.335
21	1894.5 + 342.92	1907.71 + 302.01	0.965	0.146
15mph				
7	1893.47 + 334.62	1891.85 + 239.16	0.831	0.057
13	1965.14 + 348.31	1945.18 + 288.99	0.935	0.163
28	1958.5 + 387.3	2034.07 + 320.44	0.968	0.149

Data presented as mean ± SD in Newtons (N). Correlation coefficients and effect sizes presented as point estimates

As running speeds increased, correlations for GCT fell from large/nearly perfect (8-10mph, 0.671 < r < 0.937) to ranging from small to large (11-15mph, 0.108 < r 0.879). Flight time and ST displayed a similar pattern in which relationship strength initially fell as speed increased (FT, 8-9mph, 0.741 < *r* 0.926, 10-13mph, 0.343 < *r* < 0.87; ST, 8-9mph, 0.873 < *r* < 0.945, 10-13mph, 0.246 < *r* < 0.887), before increasing again at the highest speeds (FT, 14-15mph, 0.828 < *r* < 0.907; ST, 14-15mph, 0.813 < *r* < 0.94). The relationships between force plate- and IMU-derived peak force remained very large to nearly perfect across all speeds (0.831 < r < 0.991). Robust alternatives were calculated for t-tests and effect sizes for ST to account for the violations of assumptions (**Table 3.8**).

No statistically significant differences were found between the two devices after running robust alternatives (p > 0.05; 0.000 < *ES* < 0.408). ST demonstrated following a similar pattern in relationship strength that FT demonstrated. Strength of the relationship initially fell from large/nearly perfect to a range of small/very large (8mph, *r* = 0.87 – 0.984; 9-13mph, *r* = 0.394 – 0.972), before increasing at the highest speeds (14-15mph, *r* = 0.822 – 0.982).

Table 3.8.

Robust Alternatives of Step Time for Selected Steps per Speed

Speed, Step #	Force Plate	IMU	Trimmed Mean Diff	Correlation	Effect Size
8mph					
8	330.16 ± 11.78	329.46 ± 12.21	4.337	0.984	0.213
14	331.71 ± 15.41	332.64 ± 16.07	1.163	0.932	0.046
28	333.07 ± 9.67	333.82 ± 10.96	0.070	0.870	0.009
9mph					
10	323.49 ± 12.93	323.55 ± 11.18	-0.023	0.749	0.000
12	326.89 ± 14.77	328.59 ± 12.7	0.124	0.832	0.009
27	328.4 ± 12.92	322.04 ± 12.24	7.574	0.463	0.408
10mph					
11	311.29 ± 14.68	310.08 ± 14.48	-0.733	0.521	0.037
18	321.33 ± 13.81	321.28 ± 16.97	2.661	0.664	0.151
26	319.85 ± 10	318.51 ± 14.29	4.154	0.394	0.294
11mph					
14	308.46 ± 17.27	304.79 ± 16.3	5.262	0.779	0.228
20	308.51 ± 15.78	305.73 ± 16.3	1.802	0.972	0.093
23	299.57 ± 15.45	301.94 ± 14.1	-6.174	0.718	0.228
12mph					
7	289.16 ± 12.91	294.23 ± 15.7	-6.966	0.706	0.323
15	292.62 ± 13.97	291.64 ± 13.13	3.290	0.967	0.132
29	291.01 ± 13.41	292.13 ± 11.87	-2.643	0.884	0.141
13mph					
11	282.14 ± 14.2	278.27 ± 11.83	3.417	0.572	0.162
15	283.61 ± 13.0	275.13 ± 10.97	6.669	0.426	0.416
25	281.31 ± 13.2	279.12 ± 10.65	1.571	0.865	0.094
14mph					
9	261.53 ± 21.54	261.18 ± 16.85	2.034	0.822	0.055
17	274.63 ± 17.01	267.04 ± 13.04	5.718	0.918	0.219
21	265.39 ± 22.55	266.47 ± 14.79	1.471	0.982	0.038
15mph					
7	247.94 + 17.57	248.69 + 20.24	0.042	0.972	0.000
13	266.44 + 20.51	259.08 + 24.22	8.233	0.910	0.229
28	262.68 + 28.25	262.45 + 17.81	-0.957	0.831	0.027

Data presented as mean ± SD in Newtons (N). Correlation coefficients and effect sizes presented as point estimates

Discussion

The purpose of this study was to assess the agreement of shank-mounted IMUs and force plates with estimating running temporal gait events and kinetics. When analyzing temporal gait events and kinetics averaged per speed, shank-mounted IMUs may potentially be interchangeable with force plates for measuring FT, ST, and PF. No statistically significant differences ($p < 0.05$) were presented between devices, and relationship sizes remained nearly perfect for all speeds ($r > 0.90$).

When analyzing running variables individually per step over different speeds, shank-mounted IMUs may potentially be interchangeable with force plates when estimating only peak force. Similar to averaging steps over each speed, relationship sizes were less than nearly perfect for FT and ST potentially point to less ideal interchangeability between devices, regardless of no statistically significant differences being presented. Estimating peak forces with inertial sensors has shown high levels of validity in comparison to force plates (Gurchiek et al., 2017; Setuain et al., 2018). Higher sampling frequencies with both IMUs and force plates tend to have higher levels of agreement with estimating peak forces. While placement of the sensors has typically been associated with the center of mass (COM) for estimating peak force, incorporation of the TMM could potentially produce lower levels of agreement with placement of the sensors closer to the COM.

Peak force is determined once both impulses have been summed into the resultant curve (Clark et al., 2017). One of the assumptions for the TMM is that the vertical displacement of the COM is zero throughout the whole GCT for each step (Clark et al., 2017). While the center of mass is assumed to have no changes in vertical displacement, this assumption does not include vertical displacement of the shank/heel drop at initial ground contact for forefoot strikers. One of

the main components of calculating the first impulse is the time until zero velocity of the shank/shank stabilization (Clark et al., 2017). Placement of the inertial sensors closer to the center of mass could potentially not estimate the time until shank stabilization, especially if the assumption of zero vertical displacement of the COM were true. While placement of the inertial sensors were further from the COM, calculating the impulses associated with the two different masses might produce higher levels of agreement when placed closer to the segment/joint of interest (Bergamini et al., 2012; Bergamini et al., 2013; Channells et al., 2006). With the small amount of research validating the displacement of sensors based on segmental analysis, more research should be conducted to further validate this.

Lastly, whether it is through averaging steps over each speed, or analyzing each individual step, interchangeability between shank-mounted IMUs and force plates currently might not be suited for estimating GCT. While no statistically significant differences existed between devices, correlation sizes for both scenarios were all less than nearly perfect ($r < 0.90$). One potential hypothesis for this could be that the timepoint/raw data event for toe-off might not be the true positioning for "toe-off". One potential explanation for this result could be that there are several defined moments in the raw data that have been associated with toe-off (Schmidt et al., 2016; Amman et al., 2016; Bergamini et al., 2012; Purcell et al., 2006). Different locations for placement of the sensor on the body and combinations of data used (accelerometer, gyroscope) have led to the establishment of multiple events or timepoints in the raw data potentially associated with "toe-off". Further research should assess more locations/events in raw data when using shank-mounted IMUs and combining accelerometer and gyroscope data to determine the accuracy of locating "toe-off". Further research should also analyze the differences

between skilled and non-skilled runners and the impact different foot strike patterns have on the level of agreement.

Conclusion

This study demonstrated that shank-worn IMUs are potential alternative tools in measuring both temporal gait events and gait kinetics across a range of running speeds during upright running. No statistically significant differences were found for any of the measures across both scenarios. The nearly perfect relationships and no statistically significant differences in FT, ST, and PF across averages of steps and PF across individually selected steps indicate optimistic interchangeability in some situations between IMUs and force plates when assessing temporal gait events and kinetics. Should the use of force plates not be possible, measuring GCT, FP, ST, and PF across step averages and individually selected steps from shank-mounted IMUs may provide an alternative.

REFERENCES

Al-Amari, M., Nicholas, K., Button, K., Sparkes, V., Sheeran, L., Davies, J, (2-18). Inertial measurement units for clinical movement analysis: reliability and concurrent validity. *Sensors,* 18(719),

Ammann, R., Taube, W., Wyss, T. (2016), Accuracy of PARTwear inertial sensor and Optojump optical measurement system for measuring ground contact time during running. *J. Strength Cond. Res.* 30,2057–2063.

Bergamini, E., Picerno, P., Pillet, H., Natta, F., Thoreux, P., Camomilla, V, (2012). Estimation of temporal parameters during sprint running using a trunk-mounted inertial measurement unit. *J Biomech,* 45, 1123-1126.

Bergamini, E., Guillon, P., Camomilla, V., Pillet, H., Skalli, W., Cappozzo, A., (2013). Trunk inclination estimate during the sprint start using an inertial measurement unit: a validation study. *J. Appl. Biomech*. 29, 622–627.

Channells, J., Purcell, B., Barrett, R., James, D, (2006). Determination of rotational kinematics of the lower leg during sprint running using accelerometers, in Microelectronics, MEMS, and Nanotechnology, Microelectronics, and Nanotechnology 6036, https://doi.org/10.1117/12.638392.

Charry, E., Lai, D., Begg, R., Palaniswami, M, (2009a). A study on band-pass filtering for calculating foot displacements from accelerometer and gyroscope sensors. *Engineering in Medicine and Biology,* 2009, 4824-4827.

Charry, E., Lai, D., Begg, R., Palaniswami, M, (2009b). Filtering techniques using frequency analysis for inertial sensors in gait measurements. *World Congress on Medical Physics and Biomedical Engineering,* 25(4), 1257-1260.

Clark, K., & Weyand, P. (2014). Are running speeds maximized with simple-spring mechanics? *J Appl Physiol,* 117, 604-615. doi:10.1152/japplphysiol.00174.2014.

Clark, K., Laurence, R., Weyand, P. (2017). A general relationship links gait mechanics and running ground reaction forces. *J. Exp. Biol.,* 220(2), 247-258. Doi: 10.1242/jeb.138057

Dumke, CL., Pfaffenroth, CM., McBride, JM., McCauley, GO. (2010). Relationship Between Muscle Strength, Power and Stiffness and Running Economy in Trained Male Runners. *International Journal of Sports Physiology and Performance.* 5(2), 249-61.

Hopkins, W.G., Batterham, A.M., Marshall, S.W., & Hamilton, J.J.S. (2009). Progressive statistics. 13(39), 55-70.

Giovanelli, N., Taboga, P., Rejc, E., Lazzer, S. (2017). Effects of Strength, Explosive and Plyometric Training on Energy Cost of Running in Ultra-endurance Athletes. *European Journal of Sports Science.* 17(7), 805-813.

Gurchiek, RD., McGinnis, RS., Needle, AR., McBride, JM., van Werkhoven, H, (2017). The use of a single inertial sensor to estimate 3-dimensional ground reaction force during accelerative running tasks, *J. Biomech.* 61, 263–268.

Klucken, J., Barth, J., Kugler, P., Schlachetzki, J., Henze, T., Marxreiter, F., Kohl, Z., Steidl, R., Hornegger, J., Eskofier, B., Winkler, J., (2013). Unbiased and mobile gait analysis detects motor impairment in Parkinson's disease. In: *Toft, M.* (Ed.), PLoS ONE 8(2), e56956.

Lai, DTH., Begg, R., Charry, E., Palaniswami, M, (2008). Frequency analysis of inertial sensor data for measuring toe clearance. *2008 International Conference on Intelligent Sensors, Sensor Networks, and Information Processing,* 303-308.

Macadam, P., Cronin, J., Neville, J., Diewald, S, (2019). Quantification of the validity and reliability of sprint performance metrics computed using inertial sensors: a systematic review. *Gait and Posture,* 73, 26-38.

Mikkola, J., Vesterinen, V., Taipale, R., Capostagno, B., Hakkinen, K., Nummela, A. (2011). Effect of Resistance Training Regimens on Treadmill Running and Neuromuscular Performance in Recreational Endurance Runners. *Journal of Sports Science.* 29(13), 1359-71.

Mukaka, M., (2012). Statistics corner: a guide to appropriate use of correlation coefficient in medical research. *Malawi Med J.,* 24, 69-71.

Purcell, B., Channells, J., James, D., Barrett, R, (2006). Use of accelerometers for detecting foot-ground contact time during running, *Proc. SPIE* (2006), https://doi.org/10.1117/12.638389.

Robert-Lachaine, X., Mechero, H., Larue, C., Plammondon, A, (2017). Validation of inertial measurement units with an optoelectronic system for whole-body motion analysis. *Med Biol Eng Comput,* 55: 609-619.

Schmidt, M., Rheinländer, C., Nolte, K.F. Wille, S., Wehn, N., Jaitner, T, (2016). IMU-based determination of stance duration during sprinting. *Procedia. Engin.* 147, 747–752.

Setuain, I., Lecumberri, P., Ahtiainen, J., Mero, A., Häkkinen, K., Izquierdo, M, (2018). Sprint mechanics evaluation using inertial sensor-based technology: a laboratory validation study, *Scand. J. Med. Sci. Sport*. 28, 463–472.

Zago, M., Sforza, C., Pacifici, I., Cimolin, V., Camerota, F., Celletti, C., Condoluci, C., De Pandis, MF., Galli, M, (2018). Gait evaluation using inertial measurement units in subjects with Parkinson's disease. *Journal of Electromyography and Kinesiology,* 42, 44-48.

Chapter 4. Agreement Assessment of IMU Derived Force-Time Curves Using the Two-Mass Model

AUTHOR: Smith, Austin[1]; Sams, Matt[2]; Mizuguchi, Satoshi[1]; DeWeese, Brad1; Stone, Michael[1]

AUTHOR AFFILIATIONS:

[1] Center of Excellence for Sport Science and Coach Education, Department of Sport, Exercise, Recreation and Kinesiology, East Tennessee State University, Johnson City, TN, USA

[2] Performance Science, Kansas City Royals, Surprise, AZ, USA

CORRESPONDING AUTHOR:

Austin P. Smith

East Tennessee State University

Department of Sport, Exercise, Recreation, and Kinesiology

Johnson City, TN, 37601

Phone: 804-525-8379

smithap4@etsu.edu

Shape Factor Validity of IMU Derived Force-Time Curves using the Two-Mass Model

Abstract

Force-time (F-t) curve modeling has led to advancements in running and sprinting allowing for further in-depth analysis of running kinetics. The two-mass model was developed to correct the spring-mass model's inability to reliably model force-time curves during faster velocity running and sprinting. The TMM incorporates two different impulses during sprinting, that when summed together, develop an asymmetrical curve shape properly modeling kinetics during higher velocity running. The key components of the TMM, such as ground contact time, time until shank zero velocity, shank acceleration, and body mass percentages of the two body masses utilized, have been validated using a high-speed camera setup. The purpose of this study was to validate modeling TMM F-t curves using data from shank-mounted inertial measurement units. Ten subjects completed submaximal treadmill tests with speeds ranging from 8mph to 15mph. Raw data from the IMUs were filtered and plotted manually to determine the three different temporal gait event moments. F-t curves were then approximated via previously developed TMM equations (Clark et al., 2017). Comparisons between the IMU curves and treadmill force plate curves were made by calculating 95% confidence intervals from the corrected mean differences. Comparisons were made between curves from the group as a whole, as well as sub-group analyses between skilled and recreational runners. The group-level comparison demonstrated a low level of agreement, with only 21% of the time points containing 0 in their confidence limits. Sub-group analysis found skilled runners' modeled data agreed with the

force plate across the first 63% of ground contact, whereas recreational runners' data only agreed with the force plate at peak force. The results of this study suggest F-t curves modeled from shank-mounted IMUs may possibly estimate skilled runner's F-t characteristics until the falling edge of the waveform.

Introduction

Evaluation of F-t curves and the resultant impulses underlying movement has allowed for deeper understanding of athlete movement and can serve as a potential athlete monitoring tool (Mizuguchi et al., 2015). Assessment of these parameters have allowed investigators to discern differences in shape of curves between sexes, discriminate strength levels of athletes, and contrast jump characteristics between athletes (Cormie et al., 2008; Cormie et al., 2009; Sole et al., 2018). Investigators have also examined how different training modalities can impact shapes and magnitudes of force-time curves between athletes of various strength levels (Cormie et al., 2010a; Cormie et al., 2010b).

Using more affordable equipment such as phone/camera applications and wearable sensors, force application models were developed with the goal of predicting and calculating forces and force-time curves during running without the need for expensive equipment such as force plates. The first model developed was the Spring Mass Model (SMM) (Blickhan, 1989). The SMM describes the body as a simple massless spring that compresses at touchdown, storing elastic energy, and releasing that energy during the propulsion portion of the stance phase (Alexander, 1992; Blickhan, 1989; McMahon & Cheng, 1990). While the SMM produced force-time curves during hopping and slow running were acceptable, several model assumptions led to a loss of validity when estimating forces in faster running and sprinting (Clark et al., 2014). In

brief, the model assumes the F-t curve is a half-sine in which vertical oscillation is even throughout ground contact and in which peak vertical force occurs at the midpoint of ground contact. In reality, research at faster running has shown asymmetric force application alongside peak vertical force occurring early during stance (Bundle & Weyand, 2012; Clark et al., 2014; Weyand et al., 2009). Aside from the aforementioned assumptions, the SMM was also unable to model forefoot strikers consistently (Ly et al., 2010; Zadpoor & Nikooyan, 2010).

The Two-Mass Model (TMM) was introduced as an alternative to overcome the SMM's limitations at faster running speeds. Clark and colleagues (2014) noted that the asymmetrical curve shapes and time of highest force production were different between faster and slower runners. The TMM divides the body into two masses, the first being the shank of the contact leg ($Mass_1$) and the remainder of the body ($Mass_2$) (Clark et al., 2017). Impulses are then calculated for both masses during each step, which when added together, gave a more accurate representation of force-time curves developed by faster runners.

Objectively, the TMM describes the force production in relation to the shank and the rest of the body. Using ground contact time (GCT), shank acceleration during GCT, and percent body mass of the two masses ($Mass_1$= 8%, $Mass_2$= 92%), the two impulses can be calculated representing 1) forces/impulses developed from time of initial contact until shank stabilization (impulse 1), and the forces required to accelerate the remainder of the body through the stance phase. As hypothesized by Clark and Colleagues (2017), the resultant impulse curve from the two separate impulses accurately matched curves from a treadmill equipped force plate during high velocity running. Currently, validation of obtaining the variables for the two-mass model (GCT, FT, vertical oscillation) has only been completed using high speed cameras. Therefore,

the purpose of this study is to compare the resultant impulse curves from the TMM using shank-mounted inertial measurement units to the curves from a force plate.

Methods

Subjects

Ten runners volunteered to participate in the study (5 males, 5 females, 24.5±3.6 yrs, 63.2±9.46 kg). Each subject had been actively running for at least 1 year, with past competition experience preferred. Further breakdown of subjects consisted of four recreationally trained subjects and six skilled runners (1 Olympian and 5 collegiate). Furthermore, subjects did not have any musculoskeletal injuries within the past 6 months or any other current condition that could potentially lead to complications during exercise. All subjects read and signed an informed consent document prior to participation in the study, as approved by the university's Institutional Review Board.

Data Collection

Each subject underwent one testing session in the laboratory. Subjects were first assessed for body mass measurements using a standard scale. Each subject was then prepared to run a discontinuous graded treadmill test. Inertial measurement units (Blue Thunder, Vicon Motion Systems, United Kingdom) were placed immediately superior to the medial malleolus on both shanks. Recording frequency for the IMUs was 500Hz, with data collection occurring through a smartphone application (IMU Research, 3.1, Vicon). Treadmill tests consisted of speeds 8mph-15mph, with each test lasting 20-40 seconds. Rest time between each stage lasted a minimum of 60 seconds, to allow for adequate rest to minimize the accumulation of fatigue. In addition to the IMUs, the treadmill was equipped with an embedded force plate sampling at 1000Hz. Initial

force data collection and processing was carried out in a custom LabVIEW application (LabVIEW 2018, National Instruments).

Signal Processing

Inertial measurement unit data were filtered through a second order Butterworth band-pass filter (0.7Hz to 50Hz) (Lai et al., 2008; Charry et al., 2009a; Charry et al., 2009b). Following the filter, the y-axis acceleration data, z-axis gyroscope data, and the resultant acceleration data were plotted to manually identify specific gait events. Ground Contact (GC), and Time to Zero Acceleration (T_0) were defined by the onset and termination of the first peak in the y-axis acceleration data, located in between two gyroscope peaks. Toe Off (TO) was represented as the first peak in the resultant acceleration data immediately following the highest gyroscope spike situated between the same two gyroscope peaks. These three timepoints then allowed for the calculation of Ground Contact Time (GCT), Time to shank stabilization (TSS), Flight Time (FT), and total Step Time (ST). Using the manually determined timepoints and acceleration data, $impulse_1$ and $impulse_2$, were calculated using the equations developed by Clark and colleagues (2017). Total impulse was then calculated as the sum of $impulse_1$ and $impulse_2$. Figure 5 illustrates the resulting graphs of the TMM curves from the IMU.

Figure 4.1.

Two-Mass Model impulse curve figures for 8mph and 15mph.

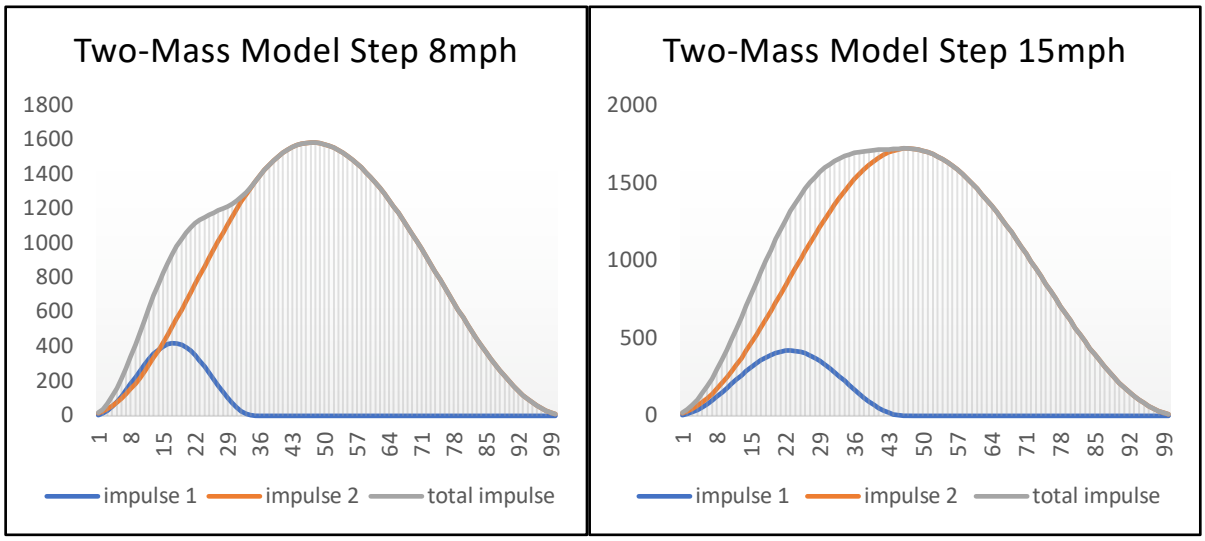

Raw data from the treadmill force plate was collected using Labview. The raw data was then integrated with the force plate calibration formula to develop raw F-t curves in a customized Rstudio application. The developed F-t curves were then filtered through a low-pass, fourth order, zero-phase-shift Butterworth filter with a frequency of 25Hz (Clark et al., 2014) in a customized R application. The first six steps of every speed for each subject were omitted from analysis to account for stabilization/proper positioning upon getting on the treadmill at each stage. Force-time curves from both the treadmill force plate and the IMUs were normalized to ground contact time, giving 100 data points for each step.

Statistical Analysis

The bias-corrected and accelerated 95% confidence intervals were calculated for the mean difference between the two devices at each of the 100 data points using ordinary non-parametric bootstrapping (2000 resamples) for the whole sample. Confidence intervals for

trimmed mean differences within each of the two different populations (skilled and recreational) were calculated using a robust paired sample t test (Mair & Wilcox, 2020) for each of the 100 data points. Because of the low sample size for both groups, bootstrapping was not possible. The confidence intervals were derived in the specific manners to avoid potential violations of general linear model. The confidence intervals were plotted to look for segments that did not include 0. A positive direction with the Cis indicated favoring of the IMUs. The segments without 0 were inferred to be statistically different. All statistical analyses were performed using the R software.

Results

Whole Group

The 95% CI for the whole running sample did not contain 0 for 79 of the 100 data points (**Figure 4.3**). The 21 data points that did contain 0 were separated into three different segments. The first and second segments did not appear to be associated with any specific event of the F-t curve, while the third segment was located at peak force of the two F-t curves.

Figure 4.2.

Force-Time curves for whole running sample from both IMUs and force plate.

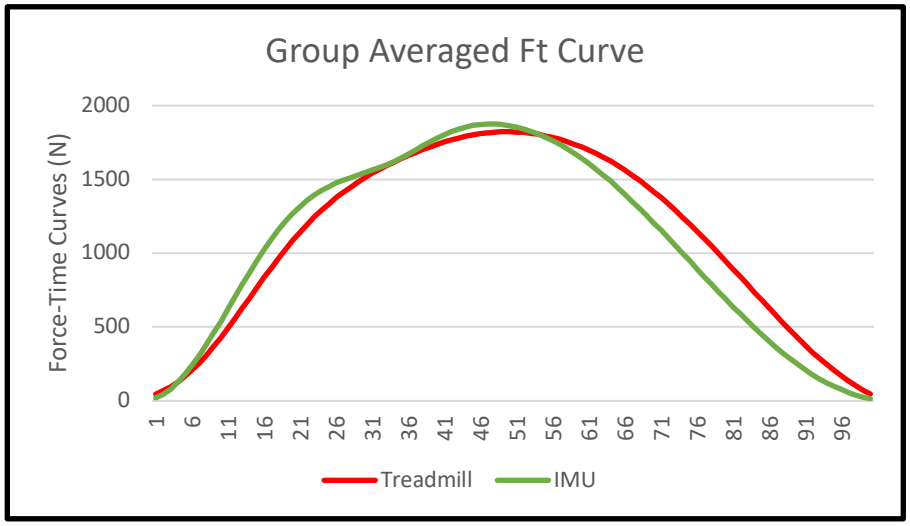

Figure 4.3.

95% CI with upper and lower limits for whole running sample F-t curves.

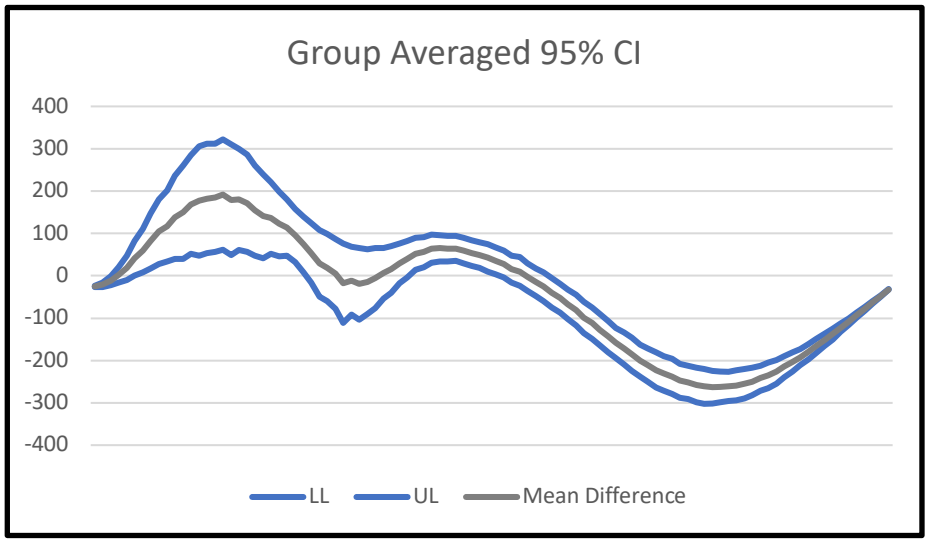

Recreational vs. Skilled Runners

The 95% CI for skilled runners contained a zero-value in the first 63 timepoints of the F-t curves (**Figure 4.5)**. The 95% CI for recreational runners did not contain a zero-value for 90 of the 100 data points (**Figure 4.7)**. The 10 data points that did contain a zero-value were separated into two different segments. The first segment of 3 timepoints did not appear to be associated with any specific event of the F-t curves. The second segment was located at the peak of the F-t curves from both devices.

Figure 4.4.

Force-Time curves for skilled runners from both IMUs and force plate

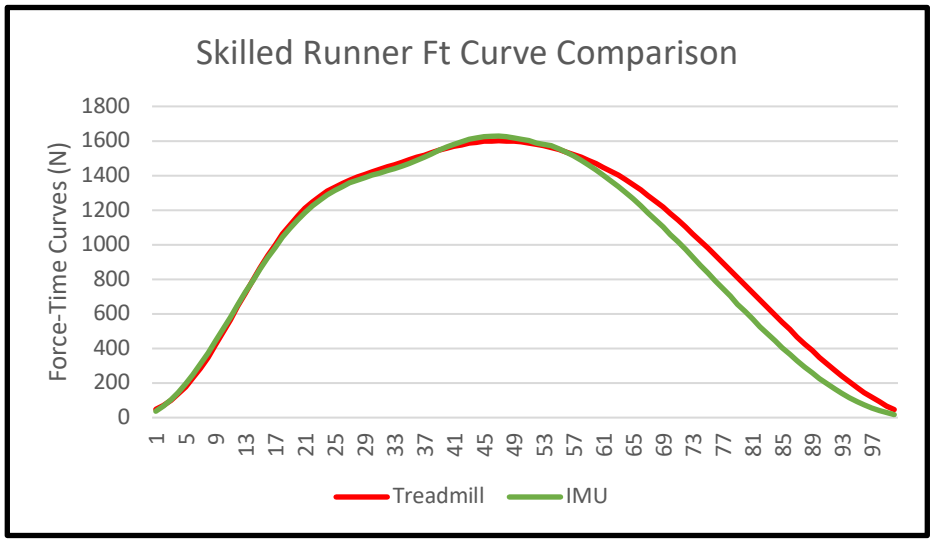

Figure 4.5

95% CI with upper and lower limits for skilled runner F-t curves.

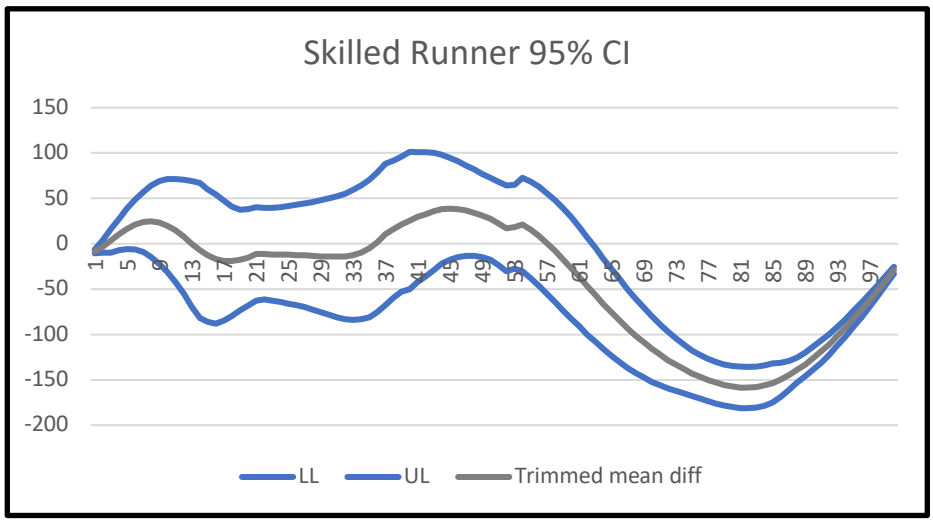

Figure 4.6

Force-time curves for recreational runner from both IMUs and force plate.

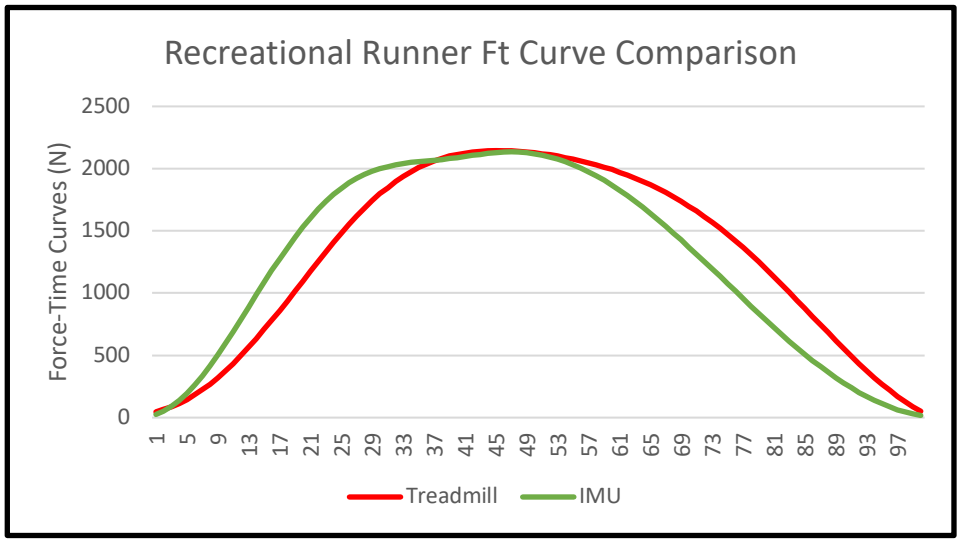

Figure 4.7

95% CI with upper and lower limits for recreational runner F-t curves.

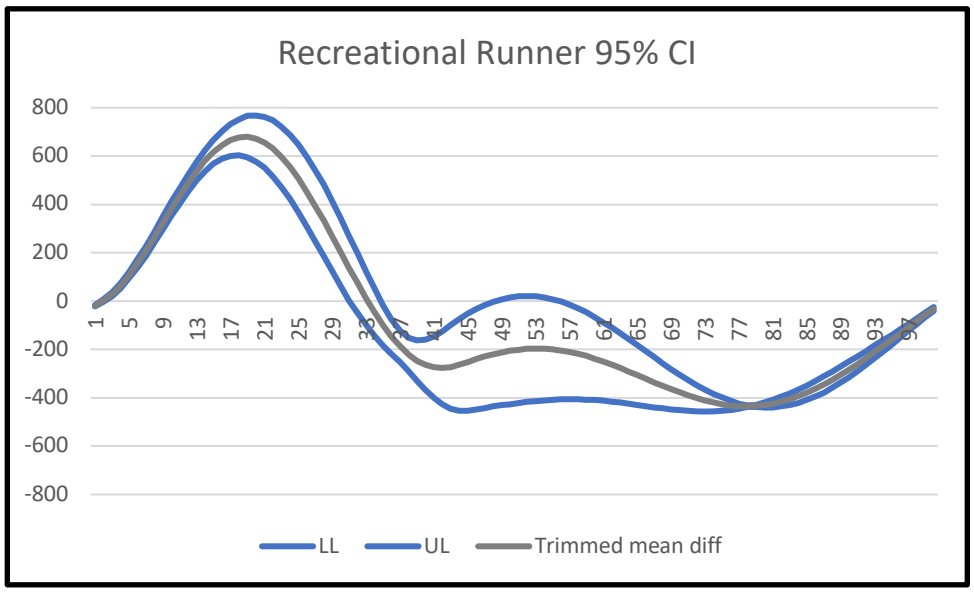

Discussion

The purpose of this study was to compare the resultant F-t curves from shank mounted IMUs using the TMM to those derived from a force plate. Force time curves derived from shank mounted IMUs may not agree with those from force plates when assessing the running sample, regardless of running skill level, and may only be practical with estimating gait events and kinetics. Seventy-nine of the 100 timepoints did not contain 0 in the 95% CI, and only one of the three portions was associated with a specific event (peak force). This agrees with the previous study (Smith et al., 2021) that indicated finding no significant differences in peak forces between the IMU and force plate.

The rising edge of the group-averaged F-t curve was higher with a steeper incline than the force plate in the first one- third segment of GCT, likely pointing to an overestimation of impulse 1. As developed by Clark and colleagues (2016) the resultant impulse curve for the TMM was calculated from the sum of impulse 1 and impulse 2. Impulse 1 is characterized as the impulse of the first mass from initial contact until the time until zero acceleration/shank stabilization (Clark et al., 2016) with one of the key variables of this calculation being the time it takes for the shank to stabilize. The need to separate skilled runners from non-skilled runners stems from the foot-strike differences between elite-level and non-elite level runners, and the differences in gait patterns that are potentially associated with those strike patterns. While most marathon runners, both elite and recreational level, exhibit rear foot strike patterns (Hanley et al., 2019; Larson et al., 2011), skilled runners and sprinters competing in events from 1500m to shorter distances more commonly practice non-rearfoot striking (Hayes and Caplan, 2012).

The IMU-derived F-t time curves from skilled runners may have a greater level of agreement than those from recreational runners. The 95% CI for the skilled runners contained

zero for the first 63 of 100 timepoints, while those from recreational runners contained zero for only 10 of the 100 timepoints. Similar to the whole group, the rising edge of the IMU resultant impulse curves from the recreational runners appeared higher with a steeper incline than the force plate, likely pointing to an overestimation of impulse 1. The first potential hypothesis to explain the overestimation of impulse 1 for the recreational runners is that heel striking could lead to larger movement artifacts than forefoot striking on initial ground contact for each footfall. Paired with this assumption is also that the company-issued ankle straps might not be able to prevent a significant amount of movement during initial contact for runners that heel strike.

The second hypothesis to explain the low level of agreement for the recreational runners' F-t curves could be that data from shank-mounted IMUs may not produce agreeable TMM-derived F-t curves. As stated previously, one of the main components for the impulse 1 calculation is the time until zero velocity, or shank stabilization (Clark et al., 2017). With heel striking, it could be likely that calculation of the time until zero velocity/shank stabilization is not possible without the use of high-speed cameras. This potential inability of the shank-mounted IMUs to calculate this variable could have been a determining factor in the overestimation of the impulse 1 for recreational runners. Further research needs to be conducted to determine the actuality of these two hypotheses.

Lastly, using high speed cameras might produce more agreeable F-t curves than shank-mounted IMUs, especially with varying skill levels of runners. As stated previously, one of the potential limitations of shank-mounted IMUs is the inability to calculate the time until shank stabilization in recreational runners/heel strikers. When using high-speed cameras, Clark and colleagues (2017) observed high levels of agreement of F-t curves with both rearfoot strikers (R^2= 0.94) and forefoot strikers (R^2= 0.95), which were observed across multiple running

velocities. Force-time curves from the high speed cameras were also able to produce high levels of agreement throughout all phases of the GCT, including the falling edge. Shank-mounted IMUs with skilled runners only produces high levels of agreement throughout the first ~60% of GCT, until after the peak and into the falling edge of the F-t curve. However, one potential limitation to the application of using high-speed cameras for the TMM is that validity has not been assessed. While very large goodness of fit values were reported with high speed cameras, the use of this statistical test does not allow for identification of specific events or portions of the F-t curve that may have exhibited low levels of agreement (Clark et al., 2017). When performing goodness of fit tests for IMU-derived F-t curves with skilled runners, very large degrees of overlap were demonstrated between the IMUs and force plate (R^2= 0.94). This did not present that the falling edge of the IMU F-t curves produced low levels of agreement according to the 95% CI of skilled runners.

While the 95% CI for the skilled runners did not contain zero for the last 37 timepoints, it does not mean that practical interchangeability is not likely between the two devices for the falling edge of the F-t curve. Effect sizes can be calculated from the mean difference of each timepoint. If the effect sizes were trivial, then interchangeability may be likely between the two devices. However, if the effect sizes are larger than trivial, it may still point to no likely interchangeability for those timepoints.

Conclusion

The purpose of this study was to assess the agreement of F-t curves derived from force plates and the TMM utilizing shank-mounted IMU data. Initial results of this study suggest that using shank-mounted IMUs to calculate TMM-based F-t curves may not be recommended

among the running sample as a whole, or for recreational runners. While less likely to produce agreeable F-t curves throughout the entirety of GCT, shank-mounted IMUs still have potential applications for use with skilled runners. The portion of the IMU F-t curves that was agreeable with the force plate was the first ~63%, which encompassed the entirety of the impulse 1 curve and the resultant peak. This can allow for higher ecological validity for research pertaining to the effect that different modalities of training (sprinting, running, weightlifting, etc.) and different sprint training tactics (incline, sled pulls, prone starts, etc.) can have on impulse 1 characteristics, vertical oscillation (time until shank stabilization), rate of force developments during initial contact, and overall peak forces

References

Alexander, M, (1992). Simple models of walking and jumping. *Human Movement Science,* 11 (1-2), 3-9.

Blickhan R. (1989). The spring-mass model for running and hopping. *J Biomech,* 22, 1217–1227.

Bundle, M., Weyand, P. (2012). Sprint exercise performance: does metabolic power matter? *Exerc. Sport Sci. Rev.,* 40(3), 174-182.

Cavagna GA, Heglund NC, Willems PA, (2005). Effect of an increase in gravity on the power output and the rebound of the body in human running. *J Exp Biol,* 208(Pt 12), 2333–46.

Charry, E., Lai, D., Begg, R., Palaniswami, M, (2009a). A study on band-pass filtering for calculating foot displacements from accelerometer and gyroscope sensors. *Engineering in Medicine and Biology,* 2009, 4824-4827.

Charry, E., Lai, D., Begg, R., Palaniswami, M, (2009b). Filtering techniques using frequency analysis for inertial sensors in gait measurements. *World Congress on Medical Physics and Biomedical Engineering,* 25(4), 1257-1260.

Clark, K., & Weyand, P. (2014). Are running speeds maximized with simple-spring mechanics? *J Appl Physiol,* 117, 604-615. doi:10.1152/japplphysiol.00174.2014.

Clark, K., Laurence, R., Weyand, P. (2017). A general relationship links gait mechanics and running ground reaction forces. *J. Exp. Biol.,* 220(2), 247-258. Doi: 10.1242/jeb.138057

Cormie, P., McGuigan, M., Newton, R. (2009). Adaptations in athletic performance after ballistic power versus strength training. *Medicine and science in sports and exercise,* 4 2(8), 1582-1598.

Cormie, Prue, MICHAEL R. McGUIGAN, and Robert U. Newton (2010a). "Changes in the eccentric phase contribute to improved stretch-shorten cycle performance after training." *Medicine & Science in Sports & Exercise* 42(9), 1731-1744.

Cormie, P., McGuigan, M., Newton, R, (2010b). Influence of training status on power absorption and production during lower body stretch-shorten cycle movements. *The Journal of Strength and Conditioning Research,* 24(1).

Cormie, P, McBride, JM, and McCaulley, GO (2008). Power-time, forcetime, and velocity-time curve analysis during the jump squat: Impact of load. *J Appl Biomech,* 24: 112

Hanley, B., Bissas, A., Merlino, S., & Gruber, AH, (2019). Most marathon runners at the 2017 IAAF World Championships were rearfoot strikers, and most did not change footstrike pattern. *J Biomech,* 92, 54-60.

Hayes, P., & Caplan, N., (2012). Foot strike patterns and ground contact times during high-calibre middle-distance races. *J Sports Sci,* 30, 1275-1283.

Larson, P., Higgins, E., Kaminski, J., Decker, T., Preble, J., Lyons, D., et el, (2011). Foot strike patterns of recreational and sub-elite runners in a long-distance road race. *J Sports Sci,* 29, 1665-1673.

Ly, Q. H., Alaoui, A., Erlicher, S. and Baly, L. (2010). Towards a footwear design tool: influence of shoe midsole properties and ground stiffness on the impact force during running. *J. Biomech*. 43, 310-317.

Mair, P., & Wilcox, R. (2020). Robust Statistical Methods in R using the WRS2 package. *Behavioral Research Methods,* 52, 464-488.

McMahon TA, Cheng GC, (1990). The mechanics of running: how does stiffness couple with speed? *J Biomech,* 23, Suppl 1: 65–78.

Mizuguchi, S., Sands, W., Wassinger, C., Lamont, H., Stone, M (2015). A new approach to determining net impulse and identification of its characteristics in countermovement jumping: reliability and validity. *Sports Biomechnics,* 14(2), 1-15.

Smith, A., Sams, M., Mizuguchi, S., DeWeese, B., & Stone, M., (2020). Validity of temporal gait events and kinetics derived from shank-mounted inertial measurement units. [Unpublished doctoral dissertation]. East Tennessee State University.

Sole, C., Miziguchi, S., Sato, K., Moir, G., and Stone, MH. Phase Characteristics of the countermovement jump force-time curve: a comparison of athletes by jumping ability. Journal of Strength and Conditioning Research, 32:4 (2018) 1155-1165.

Svedenhag J, Sjodin B, (1984). Maximal and submaximal oxygen uptakes and blood lactate levels in elite male middle- and long-distance runners. *Int J Sports Med,* 5(5), 255–61.

Weyand PG, Bundle MW, McGowan CP, Grabowski A, Brown MB, Kram R, Herr H (2009). The fastest runner on artificial limbs: different limbs, similar function? *J Appl Physiol,* 107: 903–911.

Zadpoor, A. A. and Nikooyan, A. A. (2010). Modeling muscle activity to study the effects of footwear on the impact forces and vibrations of the human body during running. *J. Biomech*. 43, 186-193.

Chapter 5. Summary and Future Direction

Shank-mounted IMUs are potentially good substitutions for force plates measuring temporal gait events and peak forces during upright running. This can be applied to both averages of steps across a similar speed and individual step analysis. When evaluating the shape factor differences of the TMM F-t curves, utilizing shank-mounted IMUs may not be valid tools when applying to a running sample as a whole when encompassing different skill levels. However, when breaking the population into recreational and skilled runners, F-t curves from the skilled runners exhibited more similarities between the IMUs and force plates and contained those similarities at key locations of the F-t graph and ground contact time. This finding suggests that the agreement of shank-mounted IMUs when incorporating the TMM is potentially dependent on the skill level of the runner. More specifically, the foot strike pattern of a runner is potentially the determining factor of producing high or low levels of agreement for IMU-derived F-t curves. While it does not produce agreeable results after the peak of the curve, skilled runners may still benefit from potential benefits of using shank-mounted IMUs that pertain to the first 63-65% of GCT.

In the future, researchers should concentrate on using more locations/events in raw data when using shank-mounted IMUs and combining both accelerometer and gyroscope data to determine the accuracy of locating “toe-off”. Additionally, researchers should also analyze the differences between skilled and non-skilled runners and foot strike patterns have on the level of agreement for temporal gait events and kinetics for individual step comparisons between devices. Lastly, researchers should assess the impact different training modalities, both general and specific to sprinting, have on the force and impulse characteristics.

References

Al-Amari, M., Nicholas, K., Button, K., Sparkes, V., Sheeran, L., Davies, J, (2-18). Inertial measurement units for clinical movement analysis: reliability and concurrent validity. *Sensors,* 18(719),

Albracht K, Arampatzis A, (2013). Exercise-induced changes in triceps surae tendon stiffness and muscle strength affect running economy in humans. *Eur J Appl Physiol.* 113(6), 1605–15.

Alexander, M, (1992). Simple models of walking and jumping. *Human Movement Science,* 11 (1-2), 3-9.

Ammann, R., Taube, W., Wyss, T. (2016), Accuracy of PARTwear inertial sensor and Optojump optical measurement system for measuring ground contact time during running. *J. Strength Cond. Res.* 30,2057–2063.

Arampatzis A, De Monte G, Karamanidis K, Morey-Klapsing G, Stafilidis S, Bruggemann GP. (2006). Influence of the muscle-tendon unit's mechanical and morphological properties on running economy. *J Exp Biol*, 209 (Pt 17), 3345–57.

Avela J, Komi PV, (1998). Reduced stretch reflex sensitivity and muscle stiffness after long-lasting stretch-shortening cycle exercise in humans. *Eur J Appl Physiol*, 78(5), 403–10.

Barnes, K., Kilding, A., (2015). Running economy: measurement, norms, and determining factors. *Sports Medicine,* 1(8), doi: 10.1186/s40798-015-0007-y

Bergamini, E., Picerno, P., Pillet, H., Natta, F., Thoreux, P., Camomilla, V, (2012). Estimation of temporal parameters during sprint running using a trunk-mounted inertial measurement unit. *J Biomech,* 45, 1123-1126.

Bergamini, E., Guillon, P., Camomilla, V., Pillet, H., Skalli, W., Cappozzo, A., (2013). Trunk inclination estimate during the sprint start using an inertial measurement unit: a validation study. *J. Appl. Biomech*. 29, 622–627.

Blickhan R. (1989). The spring-mass model for running and hopping. *J Biomech,* 22, 1217–1227.

Bobbert, M. F., Schamhardt, H. C. and Nigg, B. M. (1991). Calculation of vertical ground reaction force estimates during running from positional data. *J. Biomech.* 24, 1095-1105.

Bruggeman GP, Arampatzis A, Emrich F, Potthast W (2009). Biomechanics of double transtibial amputee sprinting using dedicated sprint prostheses. *Sports Technol,* 1: 220–227.

Brughelli, M., Cronin, J, (2007). Altering the length-tension relationship with eccentric exercise: implications for performance and injury. *Sport Medicine,* 37(9), 807-826.

Bundle, M., Weyand, P. (2012). Sprint exercise performance: does metabolic power matter? *Exerc. Sport Sci. Rev.,* 40(3), 174-182.

Cavagna GA, Sabiene FP, Margaria R, (1964). Mechanical work in running. *J Appl Physiol* 19, 249–256.

Cavagna GA, Heglund NC, Willems PA, (2005). Effect of an increase in gravity on the power output and the rebound of the body in human running. *J Exp Biol,* 208(Pt 12), 2333–46.

Cavanagh PR, Pollock ML, Landa J, (1977). A biomechanical comparison of elite and good distance runners. *Ann N Y Acad Sci*, 301, 328–45.

Channells, J., Purcell, B., Barrett, R., James, D, (2006). Determination of rotational kinematics of the lower leg during sprint running using accelerometers, in Microelectronics, MEMS, and Nanotechnology, Microelectronics, and Nanotechnology 6036, https://doi.org/10.1117/12.638392.

Charry, E., Lai, D., Begg, R., Palaniswami, M, (2009a). A study on band-pass filtering for calculating foot displacements from accelerometer and gyroscope sensors. *Engineering in Medicine and Biology,* 2009, 4824-4827.

Charry, E., Lai, D., Begg, R., Palaniswami, M, (2009b). Filtering techniques using frequency analysis for inertial sensors in gait measurements. *World Congress on Medical Physics and Biomedical Engineering,* 25(4), 1257-1260.

Clark, K., & Weyand, P. (2014). Are running speeds maximized with simple-spring mechanics? *J Appl Physiol,* 117, 604-615. doi:10.1152/japplphysiol.00174.2014.

Clark, K., Laurence, R., Weyand, P. (2017). A general relationship links gait mechanics and running ground reaction forces. *J. Exp. Biol.,* 220(2), 247-258. Doi: 10.1242/jeb.138057

Cormie, P., McGuigan, M., Newton, R. (2009). Adaptations in athletic performance after ballistic power versus strength training. *Medicine and science in sports and exercise,* 4 2(8), 1582-1598.

Cormie, Prue, MICHAEL R. McGUIGAN, and Robert U. Newton (2010a). "Changes in the eccentric phase contribute to improved stretch-shorten cycle performance after training." *Medicine & Science in Sports & Exercise* 42(9), 1731-1744.

Cormie, P., McGuigan, M., Newton, R, (2010b). Influence of training status on power absorption and production during lower body stretch-shorten cycle movements. *The Journal of Strength and Conditioning Research,* 24(1).

Cormie, P, McBride, JM, and McCaulley, GO (2008). Power-time, forcetime, and velocity-time curve analysis during the jump squat: Impact of load. *J Appl Biomech,* 24: 112

Dalleau, G., Belli, A., Bourdin, M., Lacour, JR, (1998). The spring-mass model and the energy cost of treadmill running. *European Journal of Applied Physiology,* 77, 257-263.

Daniels, J. (1985). A physiologist's view of running economy. *Med. Sci. Sports Exerc,* 17, 332-338.

Di Michele, R., Merni, F. (2014). The concurrent effects of strike pattern and ground-contact time on running economy. *Journal of Science and Medicine in Sport,* 17(4), 414-418.

Dickinson MH, Farley CT, Full RJ, Koehl MA, Kram R, Lehman S, (2000). How animals move: an integrated view. *Science*, 288: 100–106.

Dumke, CL., Pfaffenroth, CM., McBride, JM., McCauley, GO. (2010). Relationship Between Muscle Strength, Power and Stiffness and Running Economy in Trained Male Runners. *International Journal of Sports Physiology and Performance.* 5(2), 249-61.

Farley CT, Blickhan R, Saiot J, Taylor CR, (1991). Hopping frequency in humans: a test of how springs set stride frequency in bouncing gaits. *J Appl Physiol* 71: 2127–2132.

Farley, C. T., Glasheen, J. and McMahon, T. A. (1993). Running springs: speed and animal size. *J. Exp. Biol*. 185, 71-86.

Farley CT, Gonzalez O, (1996). Leg stiffness and stride frequency in human running. *J Biomech* 29: 181–186.

Farley CT, Houdijk HH, Van Strien C, Louie M (1998). Mechanism of leg stiffness adjustment for hopping on surfaces of different stiffnesses. *J Appl Physiol* 85: 1044–1055.

Ferris, DP., Louie, M., Farley, CT, (1998). Running in the real world: adjusting leg stiffness for different surfaces. *Proc Biol Sci,* 265(1400), 989-994.

Folland, J., Allen, S., Matthew, B., Handsaker, J., Forrester, S. (2017). Running technique is an important component of running economy and performance. *Medicine and Science in Sports and Exercise,* 49(7), 1412-1423. Doi: 10.1249/MSS.0000000000001245

Franklin DW, Burdet E, Osu R, Kawato M, Milner TE (2003). Functional significance of stiffness in adaptation of multijoint arm movements to stable and unstable dynamics. *Exp Brain Res*, 151(2), 145–57.

Giovanelli, N., Taboga, P., Rejc, E., Lazzer, S. (2017). Effects of Strength, Explosive and Plyometric Training on Energy Cost of Running in Ultra-endurance Athletes. *European Journal of Sports Science.* 17(7), 805-813.

Girard, O., Micallef, JP., Millet, G. (2011). Changes in spring-mass model characteristics during repeated running sprints. *European Journal of Applied Physiology,* 111, 125-134.

Gunther, M., Blickhan, R., (2002). Joint stiffness on the ankle and the knee in running. *Journal of Biomechanics,* 35(11), 1459-1474.

Gurchiek, RD., McGinnis, RS., Needle, AR., McBride, JM., van Werkhoven, H, (2017). The use of a single inertial sensor to estimate 3-dimensional ground reaction force during accelerative running tasks, *J. Biomech.* 61, 263–268.

Halvorsen K, Eriksson M, Gullstrand L, (2012). Acute effects of reducing vertical displacement and step frequency on running economy. *J Strength Cond Res*, 26(8), 2065–70.

Hanley, B., Bissas, A., Merlino, S., & Gruber, AH, (2019). Most marathon runners at the 2017 IAAF World Championships were rearfoot strikers, and most did not change footstrike pattern. *J Biomech,* 92, 54-60.

Hayes, P., & Caplan, N., (2012). Foot strike patterns and ground contact times during high-calibre middle-distance races. *J Sports Sci,* 30, 1275-1283.

He, J., Kram, R., McMahon, T, (1991). Mechanics of running under simulated low gravity. *Journal of Applied Physiology,* 71, 863-870.

Heise G, Shinohara M, Binks L, (2008). Biarticular leg muscles and links to running economy. *Int J Sports Med*., 29(8), 688–91.

Hopkins, W.G., Batterham, A.M., Marshall, S.W., & Hamilton, J.J.S. (2009). Progressive statistics. 13(39), 55-70.

Hunter, G., McCarthy, J., Carter, S., Bamman, M., Gaddy, E., Fisher, G., Katsoulis, K., Plaisance, E., Newcomer, B. (2015). Muscle fiber type, achilles tendon length, potentiation, and running economy. *J. Strength Cond. Res.,* 29, 1302-1309.

Kenneally-Dabrowski, CJ., Serpell, BG., Spratford, W, (2017). Are accelerometers a valid tool for measuring overground sprinting symmetry? *Int. J. Sport. Sci. Coach*. 13 (2), 270–277, https://doi.org/10.1177/1747954117716790.

Klucken, J., Barth, J., Kugler, P., Schlachetzki, J., Henze, T., Marxreiter, F., Kohl, Z., Steidl, R., Hornegger, J., Eskofier, B., Winkler, J., (2013). Unbiased and mobile gait analysis detects motor impairment in Parkinson's disease. In: *Toft, M.* (Ed.), PLoS ONE 8(2), e56956.

Kobsar, D., Osis, ST., Jacob, C., Ferber, R., (2019). Validity of a novel method to measure vertical oscillation during running using a depth camera. *Journal of Biomechanics,* 85, 182-186.

Komi, P, (1984). Physiological and biomechanical correlates of muscle function. *Exercise and Sport Sciences Reviews,* 12(1), 81-122.

Larson, P., Higgins, E., Kaminski, J., Decker, T., Preble, J., Lyons, D., et el, (2011). Foot strike patterns of recreational and sub-elite runners in a long-distance road race. *J Sports Sci,* 29, 1665-1673.

Ly, Q. H., Alaoui, A., Erlicher, S. and Baly, L. (2010). Towards a footwear design tool: influence of shoe midsole properties and ground stiffness on the impact force during running. *J. Biomech*. 43, 310-317.

Macadam, P., Cronin, J., Neville, J., Diewald, S, (2019). Quantification of the validity and reliability of sprint performance metrics computed using inertial sensors: a systematic review. *Gait and Posture,* 73, 26-38.

Mair, P., & Wilcox, R. (2020). Robust Statistical Methods in R using the WRS2 package. *Behavioral Research Methods,* 52, 464-488.

Mathie, MJ., Celler, BG., Lovell, NH., Coster, ACF, (2004). Classification of basic daily movements using a triaxial accelerometer. *Medical and Biological Engineering and Computing,* 42: 679-687.

McMahon, TA., Valiant, G., Frederick, EC, (1987). Groucho Running. *Journal of Applied Physiology,* 23, 65-78.

McMahon TA, Cheng GC, (1990). The mechanics of running: how does stiffness couple with speed? *J Biomech,* 23, Suppl 1: 65–78.

Mikkola, J., Vesterinen, V., Taipale, R., Capostagno, B., Hakkinen, K., Nummela, A. (2011). Effect of Resistance Training Regimens on Treadmill Running and Neuromuscular Performance in Recreational Endurance Runners. *Journal of Sports Science.* 29(13), 1359-71.

Milbrath, M., Stoepker, P., Krause, M. (2016). Video analysis tools for the assessment of running efficiency. *Track and Cross Country Journal,* 2(4), 280-283.

Miller, R., Umberger, B., Hamill, J., Caldwell, G. (2012). Evaluation of the minimum energy hypothesis and other potential optimality criteria for human running. *Proc. Biol. Sci,* 279(1733), 1498-1505. Doi: 10.1098/rspb.2011.2015

Morin, JB., Jeannin, T., Chevallier, B., Belli, A, (2005). Spring-mass model characteristics during sprint running: correlation with performance and fatigue-induced changes. *Int J Sports Med,* 27, 158-165.

Mukaka, M., (2012). Statistics corner: a guide to appropriate use of correlation coefficient in medical research. *Malawi Med J.,* 24, 69-71.

Nummela A, Kera¨nen T, Mikkelsson LO. (2007). Factors related to top running speed and economy. *Int J Sports Med*., 28(8), 655–61.

Nummela AT, Heath KA, Paavolainen LM, Lambert MI, St Clair Gibson A, Rusko HK (2008). Fatigue during a 5-km running time trial. *Int J Sports Med*.,29(9), 738–45.

Paavolainen, L., Nummela, A., Rusko, H., (1999), Neuromuscular characteristics and muscle power as determinants of 5-km running performance. *Med Sci Sports Exerc,* 31(1), 124-130

Paavolainen LM, Hakkinen K, Hamalainen I, Nummela A, Rusko H.(1999). Explosive-strength training improves 5-km running time by improving running economy and muscle power. *J Appl Physiol*., 86(5), 1527–33.

Passaro, V., Cuccovillo, A., Vaiani, L., De Carlo, M., Campanella, CE, (2017). Gyroscope technology and applications: a review in the industrial perspective. *Sensors,* 17: 2284-2306.

Pirinen, N., Pastel, M., Mykkanen, A., McGowan, C., Hyytiainen, H, (2020). Validation of tail-mounted triaxial accelerometer for measuring foals' lying and motor behavior. *Journal of Veterinary Behavior,* 39, 14-20.

Purcell, B., Channells, J., James, D., Barrett, R, (2006). Use of accelerometers for detecting foot-ground contact time during running, *Proc. SPIE* (2006), https://doi.org/10.1117/12.638389.

Robert-Lachaine, X., Mechero, H., Larue, C., Plammondon, A, (2017). Validation of inertial measurement units with an optoelectronic system for whole-body motion analysis. *Med Biol Eng Comput,* 55: 609-619.

Santos-Concejero, J., Tam, N., Granados, C., Irazusta, J., Bidaurrazaga-Letona, I., Zabala-Lili, J., Gil, S. (204). Interaction effects of stride angle and strike pattern on running economy. *Int J Sports Med*, 35(13):1118–23.

Saunders, P., Pyne, D., Telford, R., Hawley, J. (2004). Factors affecting running economy in trained distance runners. *Sports Med,* 34, 465-485.

Schmidt, M., Rheinländer, C., Nolte, K.F. Wille, S., Wehn, N., Jaitner, T, (2016). IMU-based determination of stance duration during sprinting. *Procedia. Engin.* 147, 747–752.

Setuain, I., Lecumberri, P., Ahtiainen, J., Mero, A., Häkkinen, K., Izquierdo, M, (2018). Sprint mechanics evaluation using inertial sensor-based technology: a laboratory validation study, *Scand. J. Med. Sci. Sport*. 28, 463–472.

Schutz, Y., Weinster, RL., Hunter, GR, (2001). Assessment of free-living physical activity in humans: an overview of currently available and proposed new measures. *Obesity Research,* 9(6), 368-379.

Slawinski, J., Billat, V, (2004). Difference in mechanical and energy cost between highly, well, and nontrained runners. *Medicine and Science in Sports and Exercise,* 36(8), 1440-1446.

Smith, A., Sams, M., Mizuguchi, S., DeWeese, B., & Stone, M., (2021). Validity of temporal gait events and kinetics derived from shank-mounted inertial measurement units. [Unpublished doctoral dissertation]. East Tennessee State University.

Srinivasan M, Holmes P (2008). How well can spring-mass-like telescoping leg models fit multi-pedal sagittal-plane locomotion data? *J Theor Biol,* 255: 1–7.

Svedenhag J, Sjodin B, (1984). Maximal and submaximal oxygen uptakes and blood lactate levels in elite male middle- and long-distance runners. *Int J Sports Med,* 5(5), 255–61.

Tartaruga MP, Brisswalter J, Peyre-Tartaruga LA, Avila AO, Alberton CL, Coertjens M, Cadore EL, Tiggemann CL, Silva EM, & Kruel LF. (2012). The relationship between running economy and biomechanical variables in distance runners. *Res Q Exerc Sport*, 83 (3), 367–75.

Tobin, C., Bailey, D., Trotter, M., O'Connor, L, (2020). Sensor based disease detection: a case study using accelerometers to recognize symptoms of bovine ephemeral fever. *Computers and Electronics in Agriculture,* 175

Weyand, P. G., Sternlight, D. B., Bellizzi, M. J. and Wright, S. (2000). Faster top running speeds are achieved with greater ground forces not more rapid leg movements. *J. Appl. Physiol*. 89, 1991-1999.

Weyand PG, Bundle MW, McGowan CP, Grabowski A, Brown MB, Kram R, Herr H (2009). The fastest runner on artificial limbs: different limbs, similar function? *J Appl Physiol,* 107: 903–911.

Weyand, P. G., Sandell, R. F., Prime, D. N. and Bundle, M. W. (2010). The biological limits to running speed are imposed from the ground up. *J. Appl. Physiol*. 108, 950-961.

Wittmann, F., Lambercy, O., & Gassert, R. (2019). Magnetometer-Based Drift Correction During Rest in IMU Arm Motion Tracking. *Sensors,* 19(6), 1312.

Williams, K., Cavagna, P. (1987). Relationship between distance running mechanics, running economy and performance. *Journal of Applied Physiology,* 63, 1236-1245.

Wundersitz, DW., Netto, KJ., Aisbett, B., Gastin, PB, (2013). Validity of an upper-bodymounted accelerometer to measure peak vertical and resultant force during running and change-of-direction tasks. *Sport. Biomech*. 12, 403–412.

Zadpoor, A. A. and Nikooyan, A. A. (2010). Modeling muscle activity to study the effects of footwear on the impact forces and vibrations of the human body during running. *J. Biomech*. 43, 186-193.

Zago, M., Sforza, C., Pacifici, I., Cimolin, V., Camerota, F., Celletti, C., Condoluci, C., De Pandis, MF., Galli, M, (2018). Gait evaluation using inertial measurement units in subjects with Parkinson's disease. *Journal of Electromyography and Kinesiology,* 42, 44-48.

VITA

AUSTIN PATRICK SMITH

Education:	Ph.D. Sport Physiology and Performance, East Tennessee State University, Johnson City, Tennessee, 2021
	M.S. Exercise Science, Liberty University, Lynchburg, Virginia, 2017
	B.S. Exercise Science, Liberty University, Lynchburg, Virginia, 2015
	New Kent High School, New Kent, Virginia, 2010
Professional Experience:	Strength & Conditioning Coach, Chicago Cubs, Mesa AZ, 2020-Present
	Performance Coach & Sport Scientist, USA Bobsled and Skeleton Federation, Lake Placid, New York, 2019-2020
	Instructor, East Tennessee State University, Johnson City, Tennessee, 2017-2019
	Doctoral Fellow, East Tennessee State University, Johnson City, Tennessee, 2017-2019
	Track & Field Head Strength and Conditioning Coach/Sport Scientist, Milligan University, Milligan, Tennessee, 2017-2019
	Olympic Training Site Assistant Coach & Researcher, East Tennessee State University, Johnson City, Tennessee, 2017-2019
	Biomechanics Lab Graduate Assistant, Liberty University, School of Health Science, Lynchburg, Virginia, 2015-2017
Publications:	Sato, K., Carroll, K. M., Wagle, J. P., Lang, H. M., Smith, A. P., Abbott, J. C., Hierholzer, K.M., & Stone, M. H. (2018). Validation of inertial sensor to measure velocity of medicine balls. Journal of Trainology, 7(1), 16-20.